TOWARDS INTRA-SEASONAL ESTIMATION OF FOREST NET PRIMARY PRODUCTIVITY: EVALUATING AUTOMATED DENDROMETERS FOR HIGH-TEMPORAL RESOLUTION WOODY GROWTH SIGNALS

A Thesis
Presented in Partial Fulfillment of the Requirements for the
Degree of Master of Science
with a
Major in Natural Resources
in the
College of Graduate Studies
University of Idaho
by

Jeffrey A. Stenzel

Major Professor: Tara W. Hudiburg, Ph.D.
Committee Members: Daniel M. Johnson, Ph.D.; Robert F. Keefe, Ph.D.
Department Administrator: Randy H. Brooks, Ph.D.

December 2016

Authorization to Submit Thesis

This thesis of Jeffrey Stenzel, submitted for the degree of Master of Science with a Major in Natural Resources and titled " TOWARDS INTRA-SEASONAL ESTIMATION OF FOREST NET PRIMARY PRODUCTIVITY: EVALUATING AUTOMATED DENDROMETERS FOR HIGH-TEMPORAL RESOLUTION WOODY GROWTH SIGNALS," has been reviewed in final form. Permission, as indicated by the signatures and dates below, is now granted to submit final copies to the College of Graduate Studies for approval.

Major Professor: _____ Date: _____
Tara Hudiburg, Ph.D.

Committee Members: _____ Date: _____
Daniel Johnson, Ph.D.

_____ Date: _____
Robert Keefe, Ph.D.

Department Administrator: _____ Date: _____
Randy Brooks, Ph.D.

Abstract

In the face of increased drought intensities associated with global climate change, improved understanding of forest carbon cycle responses requires novel monitoring techniques that evaluate forest processes at intra-seasonal resolutions. This study employed automated dendrometers in a northern Rocky Mountain ecosystem in order to estimate forest woody Net Primary Productivity (NPP), a carbon flux which has not previously been measured in step with ecosystem model outputs or other readily measured carbon fluxes. Site-specific patterns of multi-scale stem circumference variation in the context of summer drought stress were first characterized in order to develop a protocol for NPP estimation in dry environments. Subsequent NPP profiles were offset to later in the summer than volume growth profiles due to continual density increases and revealed species-specific timing in relation to mid-summer drought. Study findings highlighted a methodological path towards widespread implementation of more comprehensive carbon flux accounting that includes NPP estimation.

Acknowledgements

This work was supported by a graduate research assistantship through NSF Idaho EPSCoR Program and by the National Science Foundation under award number IIA-1301792. I would like to thank the College of Natural Resources for access to the University of Idaho Experimental Forest to conduct measurements. I am grateful to my major professor, Dr. Tara Hudiburg, for guidance and mentorship and my committee members Dr. Daniel Johnson and Dr. Robert Keefe for continued support. Dr. Tom Gorman was particularly generous in his contribution to the preparation of sections for x-ray density analysis. Finally, I appreciate and acknowledge my lab members and other graduate students who supported me throughout this process: Daniel Berardi, Eric Walsh, Brandon McNellis, Kathryn Baker, and Kris Daum.

Table of Contents

List of Figures

List of Tables

Chapter 1: Introduction

The Earth's 10.1 billion acres of forests account for 45% of sequestered terrestrial carbon and offset approximately one-third of yearly anthropogenic carbon emissions. As a result, forests have a profound impact on moderating rising global carbon dioxide concentrations and associated increases in global radiative forcing (*1*). Changing global climate brings with it environmental conditions and impacts on essential forest carbon cycle components that will exceed the scope of past observations, leading to significant uncertainty in regards to net effects on global forest ecosystem carbon fluxes and resulting climate feedbacks. The increasing frequency and intensity of regional drought due to increased atmospheric moisture demand is of particular concern, as drought can induce profound short and long-term disturbances in the forest carbon balance due the direct coupling of the carbon and water cycles as well as drought effects on tree mortality, insect, and fire regimes (*2–4*). Large scale, turn-of-the-century droughts in both Europe and the Western United States greatly reduced forest primary production, reducing carbon sinks to the extent that many forested areas became carbon sources to the atmosphere (*5*, *6*). Despite the pressing concern of drought effects on the global forest carbon balance (*7*), improvements in monitoring site representations of carbon flux component processes are necessary for an adequate mechanistic understanding of probable responses to unprecedented conditions. The purpose of the current study is to explore the intra-seasonal estimation of one such underrepresented component process—Net Primary Product (NPP; i.e. growth)—in the context of drought and using recent advances in automated monitoring technology.

Net Ecosystem Productivity (NEP) represents the net flux of carbon between earth and the atmosphere. Its numerical direction determines whether an ecosystem is a net atmospheric carbon source (positive) or sink (negative) and it consists of several primary component fluxes, each underlain by specific ecosystem processes (*8*). Gross Primary Production (GPP) refers to the carbon fixed by plants through the process of photosynthesis, Autotrophic Respiration (RA) is the atmospheric source of carbon that results from plant respiration (growth and maintenance related), Net Primary Production (NPP) represents plant fixed carbon remaining from respiration to be incorporated into plant structure or storage carbohydrates, and heterotrophic respiration (RH) represents the return of carbon to the

atmosphere through decomposition of organic ecosystem carbon primarily by fungi and bacteria. Currently, the standard technique for sub-daily monitoring of NEP is eddy-covariance, which measures the total flux of carbon dioxide between earth and the atmosphere. However, eddy covariance is prohibitively expensive, limited to homogenous terrain, and difficult to replicate (*9, 10*). Furthermore, eddy covariance only measures the net carbon balance, an integration of constituent fluxes; the component fluxes of GPP and Total Ecosystem Respiration (TER) are estimated quantities, while NPP is not approached (*11*). Other methods for sub-daily carbon flux component measurement typically estimate GPP or respiration but not NPP, largely due to difficulty in estimating a flow of carbon into structural or storage carbon rather than as a gaseous flux between plants and the atmosphere. Typically, NPP has instead been estimated on course temporal scales through biometric measurements that determine changes to total ecosystem stocks (mainly through volume estimations for living trees; (*12, 13*)), or modeled as the balance of other measured or modeled fluxes (e.g. (*14, 15*)). Improvements to NPP estimation that allow for in step monitoring with other carbon fluxes are currently imperative for a process-based understanding of the forest carbon cycle, both because NPP magnitude is integral in current NEP estimation and because NPP allocation dynamics have strong effects on forest physical structure and biogeochemistry (*16*). NPP wood is of particular interest, both due to its ability to be estimated from tree stem dimensions as well as it representing a large proportion of total forest ecosystem NPP (*17*). Readily employable intra-seasonal NPP estimations would serve valuable potential roles in evaluating NPP in relation to climate influences, in contrast to simply radial increment, and understanding relationships between NPP allocation and other fluxes in the context of changing climate, and assessing ecosystem model simulations of carbon allocation dynamics.

In the present study, we employ automated band dendrometers for the sub-daily (30 minute) measurement of bole circumference change, which in turn enables estimation of total stem volume growth and associated NPP_{wood}. Manually measured dendrometers have been used for many years to record stem and other tissue dimensional changes (*18*), but require regular measurement by technicians and suffer from limitations to measurement precision and temporal resolution. In recent years, automated dendrometers have been increasingly employed to provide high-temporal resolution measurements of sub-daily bole radius or circumference variations (*18, 19*). Diurnal bole circumference changes are the product of both

irreversible increases (structural growth of wood, inner bark, and outer bark tissues) and reversible, hydration related changes in the xylem and phloem (*20*). Typically, the living phloem shrinks and swells on a diurnal basis; shrinkage occurs as xylem water potential declines with daytime transpiration, while refill of depleted elastic tissue occurs at night. While both xylem and phloem can shrink and swell to some degree in relation to changing water potential, work in conifers has suggested that water storage-related dimensional changes under natural conditions (i.e. without laboratory drying) derive mostly from the phloem (*20*, *21*). Imposed atop this diel pattern is longer term increase in circumference associated predominately with secondary wood growth; daily growth is typically revealed by nighttime maximums that exceed all previous circumference values. Many previous high-resolution automated dendrometer studies have predominantly focused on the study of plant water relations (*22*, *23*) or focus on somewhat isolated characterization of the type and frequency of short term patterns across seasons (*22*, *24–26*). Others have related integrated growth and circumference signals in relation to other [non NPP] explicit ecosystem carbon fluxes (*27*, *28*). The goal of this study is to examine the use of automated dendrometer circumference variations to infer intra-seasonal woody growth dynamics with the goal of then estimating NPP (from calculated biomass increment) at the stand level. In contrast to studies that have sought to elucidate physiological patterns of individual trees, we employ affordable band dendrometers whose related high replication could allow for ecosystem level assessments of intra-seasonal NPP, particularly in the context of increasing drought. Furthermore, many previous studies that have investigated radial or circumferential variation have done so in temperate European forest ecosystems, resulting in examination of stem size variations in the absence of regular, severe soil moisture deficit (*27*, *29*). Because dendrometer signals integrate both growth and hydration signals, examining how drought-prone conditions might influence circumference variations serves as a necessary step towards evaluating ecosystem NPP responses to intensifying drought regimes associated with climate change.

The following pages are divided into two primary chapters, focusing on site specific characterizations of dendrometer circumference variations collected at a mixed conifer forest with seasonal drought (Chapter 2) and on the results of an implementation of a suite of

methods necessary for estimation of intra-seasonal NPP_{wood} from dendrometer circumference patterns (Chapter 3).

In Chapter 2 (Site and dendrometer characterization), the first objective is to delineate the primary periods of distinct stem circumference variation patterns across the year (circumference pattern "seasons"), how those periods interrelate, and during which periods information relevant to woody circumference growth may be derived. The other primary objective of this section is to evaluate the degree to which growing season circumference variations are able to provide reasonable agreement with signals expected from secondary woody growth. Briefly, expectations for a woody growth signal include consistent cumulative growth across days which follows an approximately sigmoidal shape (*13*, *30*). Such growth is characterized by rapid initiation of growth in the Spring; a single period of consistent growth; and a relatively gradual cessation of circumference growth that is associated with end-of-season environmental stresses, decreasing tracheid dimensions, and finally, decreasing cell production rates from the vascular cambium. Circumference decreases are not indicative of the accumulation of permanent rings and wood radius, and instead show localized dominance of elastic changes associated with variable hydration of bark tissues (*20*). Additionally, though it is possible for cell expansion or wall deposition rates to vary within the growing season, we expect growth to conform to a sigmoidal shape due to a significant degree of dependence of current rates of woody growth on total numbers of cells in the expansive phase a xylogenesis, which is partially determined by cambial activity occurring days to weeks in advance (*31*).

In Chapter 3 (Woody NPP characterization), the primary objective is approach NPP_{wood} estimation in a manner consistent with the circumference variation insights highlighted in Chapter 2. This entails applying reasonable extraction constraints on circumference variations to ensure that transformed signals represent woody growth, rather than bark hydration changes. Furthermore, this chapter includes a method for estimating and aligning intra-seasonal wood density, the necessary scalar for a mass estimation (i.e. NPP). The final objectives of this section are to evaluate the profiles of estimated NPP throughout the season, including comparisons to circumference or volume-only profiles, comparisons between tree species, and timings in relation to key ambient conditions.

Chapter 2: Site and dendrometer characterization

Methods

Location: Research plots were located in a mixed conifer stand in the University of Idaho Experimental forest. Following an early 20th century clearcut harvest, natural regeneration has since resulted in a dense stand consisting predominantly of Western redcedar (*Thuja plicata*), Douglas fir (*Pseudotsuga menziesii*), Grand fir (*Abies grandis*), and Western larch (*Larix occidentalis*), with scattered relic Douglas fir, Ponderosa Pine (*Pinus ponderosa*), and Western White Pine (*Pinus monticolla*). With the exception of intermittent, suppressed Western redcedar and areas adjacent to gaps, the understory is largely clear of live vegetation.

The forest falls within the Idaho Northern Rocky Mountain region (46.80, -116.81, elevation=1050m) and experiences a dry-summer continental climate (Dsb), characterized by cold, wet winters and extended summer drought. Average yearly temperature and precipitation are 7.4° C and 810mm, respectively, with less than 5% of yearly precipitation typically falling during the summer months (JJA).

Dendrometer Bands: TreeHugger automated dendrometer bands (Global Change Solutions, LLC) were installed on 54 mature trees by March 2015, approximately two months prior to typical growing season initiation. Installation was based around an existing 6 acre experimental plot design, with Treehuggers equally distributed within 24 subplots and installed on trees nearest to subplot centers. TreeHugger dendrometer bands record bole circumference changes via shifting stylus depression of a soft potentiometer pad. Dendrometer accuracy is ±10μm and measurement resolution is 6 μm. Prior to installation, outer stem bark was smoothed with a rasp and chisel when needed due to surface irregularity. Smoothing was most extensive on Western Larch and Western redcedar due to respectively irregular corky and fibrous bark. Bands were installed approximately at breast height (1.37m) and appropriate spring tension for proper stylus-potentiometer overlap was verified. Circumference and band/logger temperature were recorded at 30 minute intervals by a dedicated logger associated with each band. Data was manually retrieved from loggers and copied from logger SD memory cards.

Manual band dendrometers were installed on a total of 100 stand trees, including all trees with automated dendrometers. At 2 week intervals during 2016, changes in circumference (mm) were measured with digital calipers (0.01mm resolution). 2015 measurements were performed prior to and after the termination of the growing season.

Ambient Conditions: As a result of study site power failures, environmental variables for 2015 and 2016 year descriptions are gathered primarily from the Moscow Mountain Snotel Station (Natural Resources Conservation Service (NRCS)), which is located approximately 3km from the study stand. The Snotel station location is on the same ridge as the study site (Moscow Mountain) and within a similar forest composition. Snotel variables used in this study include daily air temperature, soil moisture (2, 8, & 20cm), soil temperature, precipitation, and snow depth. To compare recent years' conditions to historical climate, WestWide Drought Tracker (online tool; University of Idaho and Desert Research Institute) was employed to query and visualize interpolated PRISM climate products (*32*). In addition to site and regional temperature and precipitation, several calculated drought metrics were examined, both driven by temperature and precipitation inputs; The Self-Calibrated Palmer Drought Severity Index (scPDSI) is a locally calibrated calculation of water budget that reflects >12 month conditions; The Standardized Precipitation Evapotranspiration Index (SPEI) calculates monthly drought status.

Data Management and Analysis: Nearly half of the installed dendrometer bands were destroyed or severely disrupted by bear activity in the stand. Of the remaining functional bands, several forms of erroneous readings were screened. While periods of exceptionally rapid expansion were common during spring rain events, daily expansions exceeding 0.5 mm day $^{-1}$ were removed; such offsets were associated with user or wildlife activity that directly shifted the band stylus. Individual outliers (<0.5 mm from local medians) associated with resets or occasionally equipment error were generally deleted using the "hampel" function of R package "pracma".

Because the focus of this study was on irreversible structural growth at a daily scale, hydration-related daily oscillations in circumference were removed with a smoothing spline; "smooth.spline()" function (base R) was employed and degrees of freedom were set to the

number of recording days in order to produce daily smoothed circumference traces for each band/tree. This transformation also served to reduce the effect of remaining low-magnitude errors which were not screened with the initial screening procedure.

From the smoothed growth series, phenological stages were extracted throughout the season (see Figure 2.14). Due to intermittent small variations in circumference associated with freeze-thaw, rain events, and unaccounted disturbance, growth initiation was classified as the time of year at which 5% of yearly total growth was achieved. Due to the yearly idiosyncratic patterns of seasonal circumference change discovered at the study site (details below), yearly starting values were assigned to the springtime minimum of each series. Spring minimum circumferences were defined as the minimum points prior to the yearly growing period and after (only in 2016) the previous winter maximum (between November and April). Summer maximum circumferences were assigned to peak circumference values prior to September 1st of each year. The September growing season boundary was assigned with reference to relevant literature that detailed end dates of stem circumference change or xylem development in Douglas fir (*30, 31*), the most xeric species studied and the species that presumably is capable of continuing growth latest into the summer drought period. Furthermore, examination of the primary growing season off all individuals at the field site revealed that all trees ceased detectable growth before September. Fall rewet circumferences were determined at points of maximum circumference change deceleration during the rapid expansion phase associated with rapid Fall rehydration of soils. Summer minimum circumferences were defined as minimum tree circumference between summer maximum and fall rewet circumference. Winter maximums were defined as maximum circumference during the winter months, and were found between summer and spring minimums.

Further analysis was performed on growing season circumference variation by transforming data to only allow circumference increases, thus creating stepped, accumulated growth profiles which displayed combinations of growth and static circumference. To examine daily-spline variations against mid-term variations (10-days), 10-day splines were created from individual dendrometer traces (degrees of freedom equal to the number of 10 day periods per series).

All Data transformations and statistical analyses were performed in R Version 3.2.1 (*35*).

Results

Climate: 2015 was defined by record setting temperatures, below-average precipitation, and resulting severe drought in much of the Northwest U.S. (Figure A.1). At the study site, monthly average temperatures were above normal through October (exceptions: April, September), with exceptional temperatures in June 2015 (Figure A.2, Figure 2.3). Early growing season precipitation was intermittent; April experienced exceptionally low early-season precipitation, while rainfall exceeded normal in May. June through October precipitation was below normal (Figure A.2, Figure 2.2). As a result of high temperature and low precipitation, calculated monthly drought indices indicated extraordinary drought, particularly in the summer months (JJA), April, and October (Figure A.3). Rooting depth soil moisture measurements (20cm) are available from the nearby Moscow Mountain Snotel station since 2006. From this record period, 2015 demonstrated the longest period of summer with VWC <5% on record at 101 days, approximately two times the 15 year mean. 0. 5% VWC, the approximate soil dryness at which wilting point conditions can be inferred, was reached at the 20cm depth by July 24th, about one month before normal. Soil moisture decline was pronounced in April, though significant recharge (i.e. a large, rapid increase in measured VWC) occurred in May. From the last recharge event on June 3rd, 20cm VWC declined to 5% in 51 days (July 24th; -0.49% VWC day^{-1}). Rapid VWC recharge began on November 1st (Figure 2.1).

Maximum Snotel site snow depth in the winter months of 2015 was 26 inches; the first date at which snow depth was zero was March 21st, while the date after which no further seasonal snow accumulation occurred was April 8th (Figure 2.5). Soil temperature (Snotel) rose relatively gradually beginning in mid-March, with rooting zone temperatures exceeding 5° C between April 18th (2cm depth) and May 4th (20cm depth:Figure 2.4). Daily minimum Snotel air temperature did not fall below 0° C after April 23rd and did not decrease below 5° C after May 14th (Figure 2.3).

2016 was characterized by intermittent dry months, but was less extraordinarily hot than 2015. Summer temperatures were near-normal, while January through April temperatures were moderately above normal (Figure A.2, Figure 2.3). Growing season

months (April through September) experienced near normal precipitation, with below normal months falling within the 2nd quartile (Figure A.2, Figure 2.2). Monthly drought indices (e.g. monthly SPEI) demonstrated a mix of above and below normal months (Figure A.3). However, accumulated drought indices (e.g sc-PDSI) through September indicate that 2016, though less extreme than 2015, was still relatively dry and influenced by preceding drought conditions (Figure A.3). In the late year, an exceptionally wet October abated a several year pattern of decreasing and negative scPSDI values. Snotel soil moisture demonstrated a much shorter period of <5% volumetric soil moisture in comparison to 2015, lasting from August 28th to October 11th (46 days, 20cm depth). Rooting zone (20cm) soil moisture decline began in mid-April and was partially recharged in May. Continuous growing season VWC decline (20cm) began after May 24th and was more moderate than in 2015. 5% VWC was reached on August 28th (96 days; -0.26% VWC day^{-1}). Fall soil recharge occurred in early October, nearly a month before recharge in 2015 (Figure 2.1).

Maximum Snotel snow depth in the winter months of 2016 was 57 inches and the date of zero depth was April 21st (Figure 2.5). Soil temperatures rose abruptly in relation to 2015, with heating beginning in mid-April following snow melt. 5° C temperature thresholds were exceeded between April 21st (2cm) and May 6th (20cm) (Figure 2.4). Daily minimum air temperature did not fall below 0° C later than April 8th, while occasional nights with temperatures below 5° C were experienced as late into the growing season as June 25th (Figure 2.3).

Circumference Change Characterizations - General Site Patterns: The study site growing season was characterized by rapid growth initiated at a similar date across individuals per year, a rapid decline in growth rate between July and August, and a period of mid-summer shrinkage or, in exceptional individuals, quiescence (Figures 2.6-2.9). Notably, the rapid growth period was characterized by varying degrees of strong, multi-day heterogeneity associated with precipitation events (Figures 2.12, 2.13, see Heterogeneity results below); such events were associated with highly increased expansion rates and were often followed by multiple days of greatly diminished expansion or circumference shrinkage. The “summer deficit” period ended upon the return of soil-wetting precipitation in Fall and was accompanied by extremely rapid (several day) and large (millimeter scale) circumference

expansion that typically exceeded the current year's summer maximum. Subsequent to rapid refill, most individuals demonstrated consistent, slow expansion across the course of the winter that was punctuated by freeze-thaw fluctuations. Notably, while winter was characterized by several short periods of large, freeze-thaw associated bole circumference variation, no periods of consistent winter shrinkage (approximately November-April) and subsequent spring refill (approximately March-April) were depicted.

General Species Patterns: Species-specific patterns of circumference variation were visible at this study site. General species differences will be relayed in this section, while statistical assessment of characteristics will follow below.

Western larch individuals were ultimately excluded from much of the subsequent growth analysis due to an apparent lack of detectable growth in most individuals. Larch trees displayed exceptionally low crown mass, infestation by dwarf mistletoe, and wind damage. Additionally, stand conditions were significantly denser than the open conditions that typically favor this early successional species. Yearly positive growth was not detected for most larches observed. Manual bands demonstrated static or net negative yearly values; automated dendrometers indicated rapid positive change during spring rains that typically fell below the spring minimum during the summer, resulting in net negative circumference change. Wood cores demonstrated year to year increment that was not consistently able to be differentiated due to growth of only one to four tracheids per year. Such tracheid counts eliminated the normal earlywood-to-latewood density gradient that allows for distinct separation and measurement of years.

Douglas fir and Grand fir demonstrated similar seasonal circumference patterns, with relatively consistent growing season increases in circumference that were not excessively punctuated by short-term circumference fluctuations (Figure 2.10 for Douglas fir). Summer shrinkage was generally apparent for both Douglas fir and Grand fir, though to a lesser extent than other species. Similarly, the positive offset associated with fall rewet was apparent yet relatively small. A distinguishing feature of Douglas fir in particular was a slow, consistent increase in circumference throughout the winter that resulted in a subsequent spring minimum that exceeded summer or fall maximums from the previous year.

Western Redcedar was characterized by greater mid-term reversible variation (days to weeks) than the non-Larch species, both during the growing season and winter (Figure 2.10). During the growing season, rain events resulted in millimeter-scale circumference increases within hours to days; however, the days following these rapid expansions were characterized by circumference decreases and/or growth rates that fell below pre-rain values. The resulting heterogeneity of growing season growth rates appears as a distinctly stepped pattern (Figure 2.10). Summer shrinkage was pronounced, while fall rewet typically elevated circumference well above previous maximums. While slow, long-term winter expansion was apparent, this expansion was reversed by a Spring shrinkage (mm magnitude) to a pre-growing season spring minimum circumference.

Circumference Variation Metric Analysis: Robust quantification of seasonal variation metrics by species was inhibited by considerable loss of functional equipment during the initial season. Due to resulting low sample sizes, statistical comparisons were performed only for Douglas fir and Western redcedar for 2015 and 2016.

In 2015, key differences were detected between the magnitudes of species summer deficit (shrinkage), rewet expansion, rewet to spring expansion, and spring shrinkage (Table 2.1; reported metric t-test p-values <0.05). Differences were also apparent between proportional measures of summer to rewet maximums, rewet to spring minimums, and winter maximums to spring minimums. As a reference variation to the following metrics, average yearly circumference growth across non-larch species was 8.2mm (1.3mm radial increment). Western redcedar average summer shrinkage was over double that of Douglas fir, at 1.3mm vs 0.6mm. Compensating for this circumference decrease, cedar rewet circumference increase over previous summer maximum was also greater than Douglas fir (1.1mm vs 0.7mm). While both species displayed circumference increases over the course of the winter (mean=2.1mm), prominent winter shrinkage led to lower increases in rewet to spring minimum circumference in cedar than in Douglas fir (0.2mm vs 1.4 mm). Spring shrinkage averaged 1.8mm for cedar and 1.2 mm for Douglas fir. For cedar, average summer maximum circumference was 81% of rewet circumference, rewet circumference was 97% of the subsequent spring minimum (i.e. yearly total growth), and spring minimum was 81% of the winter maximum. For Douglas fir, average summer maximum was 95% of rewet circumference, rewet circumference was 82%

of spring minimum, and spring minimum was 96% of winter maximum. Cedar growing season maximums therefore tended to underestimate yearly total growth, but most of yearly growth was apparent by the Fall rewet period. In contrast, Douglas fir summer maximums represented a relatively high proportion of total yearly growth, yet relative Fall underestimates meant that circumference growth continued to approach the yearly total through the length of the winter. In 2016, measurements were only available through the Fall rewet period. Of the possible comparisons, key differences were only apparent in species summer circumference deficits, which continued to be much greater in cedar than in Douglas fir (2.0mm vs 1.2 mm; Table 2.2).

Nine trees had complete records for the 2015 and 2016 growing season; due to this low sample number, yearly differences between seasonal metrics were not statistically assessed on a species basis. Of the measures examined on a species basis above, none were significantly different across species in 2015 compared to 2016. However, total circumference change until summer maximums was greater during 2015 than 2016, with mean circumference growth rates (during the period of growth between 5% and 90% of summer maximum) of 0.135 and 0.111 mm day^{-1}, respectively (paired t-test, $p<.01$). In comparison to 2016, higher average growth rates were displayed in 2015 in all trees that had complete measurements during both years. Though total yearly growth was not different between years, growing season lengths were; average time between 5% and 90% of summer maximum circumference growth was 55 days in 2015 and 72 days in 2016 (paired t-test; $p<.001$). The average date at which 5% of summer maximum circumference growth was reached was May 11th in 2015 and April 29th in 2016, while the average date at which 90% of summer maximum circumference was reached was July 6th in 2015 and July 10th in 2016 (paired t-test, $p< .0001$ and $p<.05$). In 2015, the ranges for 5% and 90% growth dates among individuals were 16 and 19 days. In 2016, the ranges for threshold dates were 8 and 18 days. In 2015, the first half of the 5%-90% growth period demonstrated an average of 190% the growth of the second half (paired t-test, $p<.05$). In 2016, the first half of the period exhibited 104% of second half growth (paired t-test, $p=0.94$). This appeared as relatively constant growth during most of the 2016 growing period and as continuous decline in growth from an early growing season maximum rate in 2015 (Figures 2.6-2.10).

On average, the period between 90% of yearly circumference growth [to summer maximum] and summer maximum was 16 days in 2015 and 24 days in 2016. In 2015, this period was characterized by continuous expansion to summer maximum circumference followed by immediate circumference decrease (entrance into the summer deficit period; Figures 2.6, 2.7). In 2016, this time consisted of a short period of continued rapid growth (up to approximately 95% of summer maximum) followed by a period of relatively static circumference prior to summer shrinkage (Figures 2.8, 2.9).

The summer deficit period was defined as falling between summer maximum circumference and Fall rewet circumference maximum. The average deficit period was 106 days in 2015 and 68 days in 2016, a 38 day difference (paired t-test; $p<.001$). The deficit period was briefly interrupted by an isolated rain event in September, 2015, which resulted in temporary and partial circumference recovery and shallow soil moisture recharge.

Growing Season Circumference Change Heterogeneity: Several additional analyses were employed to explore the high, rain associated variability in growing season circumference patterns. Because post-rain event rapid expansion was often followed by static or decreasing circumference the binary daily growth status (daily growth vs no growth) of all individuals was examined. Our pre-measurement hypothesis regarding growing season growth was that intra-seasonal rates would vary but remain positive between a spring minimum and summer maximum (the primary growing season). The average number of days displaying growth during the 2015 main growing period (5% to 90% of maximum summer growth) was for all individuals 44 of 55 days (79%), for Western redcedar 37 of 52 days (73%), for Grand fir 48 of 56 days (85%), and for Douglas fir 54 of 61 days (89%). Differences in growing season growth day proportions between Western redcedar and Douglas fir were not significantly different, though differences in total number of days with growth were (t-test, $p<.05$). In 2016, average number of growth days for all trees was 58 of 80 days (74%), for Western redcedar was 49 of 75 days (66%), for Grand fir was 77 of 87 days (88%) and for Douglas fir was 60 of 83 days (77%). While the average proportion of growth days was greater in 2015 than 2016, matched tree differences were non-significant (paired t-test, $p>.05$).

Variation in growth was further examined on a species basis by examining proportions of each species that exhibited growth on each day. Across both Western redcedar and Douglas

fir, the longer growing season of 2016 was apparent in proportion plots (Figure 2.11). Both 2015 and 2016 demonstrated variable proportions of growth during the peak growing season, with one period and two periods of considerable proportion decline (-70-80%) during 2015 and 2016, respectively. In both 2015 and 2016, Western redcedar deviated from ubiquitous growth (100%) to a greater extent than Douglas fir, though this trend is more pronounced in 2015. In 2016, mean peak season proportions for Douglas fir and Western redcedar were 0.80 (±0.31) and 0.66 (±0.22) (paired t-test, $p<.001$), consistent with lower proportions of Western redcedar growth days and greater variability. In 2015, mean peak-period proportions were 0.86 (±0.11) for Douglas fir and 0.62 (±0.23) for western redcedar (paired t-test, $p<.001$).

The following values are presented as a percentage of total summer growth per measurement interval (30 minutes). In 2015, species average maximum and mean growing period growth rates were 0.22% and 0.032% (±0.05) for Western redcedar and 0.08% and 0.024% (±0.017) for Douglas fir per interval, highlighting the rapid, rain-related deviations [expansion followed by shrinkage] displayed by cedars. In 2016, lower summary rates were recorded; maximum and mean growth rates were 0.11% and 0.025% (±0.025%) for Western redcedar and 0.07% and 0.018% (±0.017%) for Douglas fir. To further examine short term circumference variation against mid-term trends, species average growth rate traces were compared to 10-day growth rate splines. Deviation plots, indicating differences between species daily rates and mid-term patterns (10-day splines), highlight pronounced cedar rate deviations during early summer rain events (Figures 2.12, 2.13). These deviations were particularly apparent in the early growing season (May-June) of 2015, and dominated the high mean and maximum deviations exhibited by cedar. High deviations coincided with intermittent periods defined by heavy rain (see Figures 2.2, 2.12), and demonstrate high short term circumference variability. In 2015, mean deviations were 0.009% (± .008%) for PM and 0.020% (±.029%) for TP. R-squared values for Daily and 10-day splines were 0.64 (PM) and 0.36 (TP). In 2016, mean deviations were 0.008% (±0.008%) for PM and 0.015% (±0.013) for TP. R-squared values between splines were 0.57 (PM) and 0.51 (TP), demonstrating that, while fits between daily and 10 day values were less divergent between species in 2016, cedar continued to demonstrate more extensive daily-scale variability.

Manual Dendrometer Bands: Manual band measurements were taken at approximate two week intervals throughout the 2016 growing season and were available from 82 trees of the three species analyzed with automated dendrometers (Douglas fir, Grand fir, Western redcedar).

Manual band mean summer maximum circumference growth was 7.23mm (± 4.32mm), mean summer shrinkage was 1.01 mm (± 0.63mm), and mean expansion above summer minimum detected immediately after fall rewet (measurement on 10/12/2016) was 2.28 mm (±1.11). Average total circumference increase from summer maximum at Fall rewet was 1.26 mm (±0.73), while average total growth through rewet of 8.69 mm (±4.31mm). Mean shrinkage as a proportion of summer maximum was 21% (sd= 21%). Post-rewet yearly circumference growth was on average 24% (±24%) of total growth through summer max.

In contrast to findings from automated dendrometer data, statistically significant differences were detected between species circumference change metrics of trees with manual dendrometers. Significant inter-species differences in summer maximum circumference growth, summer shrinkage, fall expansion (from summer minimum and summer maximum), shrinkage as a proportion of summer total growth, and rewet circumference increase as a proportion of summer maximum circumference growth were detected (one-way ANOVA, $p < .05$ for all metrics). On average, Western redcedar displayed lower summer maximum growth, greater summer shrinkage, and greater rewet expansion than Douglas fir and Grand fir, with consistent statistical differences detected between species pairs (Tukey HSD, p-values<.05). Douglas fir growth metrics and circumference variability were greater than those of Grand fir on average, though species differences were not significant. In contrast to summer maximum circumference change and variability metrics, post-rewet total yearly circumference growth (absolute) was not significantly different between species (one-way ANOVA, $p > .05$).

Measurement dates at which maximum yearly circumference growth through summer was detected ranged from July 6th through August 29th, with the majority of maximums falling on July 21st and August 15th (58% and 29% respectively). Species differences were largely responsible for these two common maximum dates; 77% of Western redcedar displayed summer maximums on July 21st and 67% of Douglas fir displayed maximums on August 15th. Grand fir displayed an equal proportion of maximums on both dates (41% of individuals on each date).

Increment Cores: Significant species level differences were found in 2015 core increments (ANOVA, $p<.05$; Tukey HSD: TP-PM, $p<.05$). Average 2015 core increments for Grand fir, Douglas fir, and Western Redcedar were 1.80mm, 2.21 mm, and 1.52mm, respectively. Significant species-level differences between 2016 wood core increments were not detected. Mean core increment during 2016 was 1.40 mm for Grand fir, 1.81 mm for Douglas fir, and 1.51 mm for Western redcedar. Mean increment was 0.18mm less in 2016 than in 2015 (1.75 mm in 2015, 1.56 mm in 2015; Paired t-test, $p<.01$). Decreases in mean values occurred for every species but were pronounced in Grand fir and Douglas fir (species-specific paired t-test ABGR: $p<.01$; PSME: $p=.07$).

Method Comparison: Manual band post-rewet total circumference change was an average of 6.19 times (±2.71, IQR= 4.6-6.9) 2016 core increment (Adjusted R-squared= .91). Given the geometric relationship between circumference and radius for [assumed] circular stem cross sections, the expected coefficient is a similar 6.28. Mean 2016 automated dendrometer circumference growth (total) was 6.47 times the mean matching core increment (Adjusted R-squared= 0.87). Mean 2015 automated dendrometer growth was 5.31 times the mean matching core increment. (Adjusted R-squared: 0.89)

On trees with matching automated and manual dendrometer bands, mean automated band circumference growth through 2016 Fall rewet was 10.22 mm (sd=5.10) while mean manual band growth through the post-rewet measurement was 10.18 mm (sd= 4.47 mm) (Adjusted R-squared = 0.98, n=14).

Discussion

The most novel element of the UIEF automated dendrometer data set was the site-specific inter-seasonal circumference variation pattern, which stands in contrast to most reported seasonal progressions to date. Many previous dendrometer studies (automated and manual) have been performed in forests that are not characterized by summer drought and corresponding severe soil moisture deficit (*27*, *36–39*). Studies typically report seasonal variation stages which exhibit essential differences from the patterns seen in this northern Rocky Mountain forest. Previously described patterns include comparatively consistent

positive change (i.e. growth) through the warm season which tapers but does not reverse through the Fall; winter is then characterized by intermittent fluctuations associated with the freeze and thaw of internal moisture as well as winter-long desiccation associated with impaired water uptake combined with continued low-level transpiration. Finally, following such pronounced cold-season shrinkage, Spring growth is preceded by an expansive rehydration period. While degree of variation per period varied across the conifer species found at this study site, an idiosyncratic common site pattern was found (Figures 2.6-2.9). First, spring growth initiation in both years was preceded by an early-spring shrinkage period. Subsequent warm season growth was interrupted by July or August with a pronounced summer shrinkage period, though near-static late-summer circumference was apparent in a few, fast growing individuals (Figures 2.6 and 2.8). Calculation of total growing season woody growth was then complicated by an immediate, rapid period (hours to days) of circumference increase that exceeded growth rates observed during the main growing season. Winter was typically marked by continued gradual circumference increase punctuated by occasional freeze-thaw fluctuations. While the pattern observed at the UIEF site is not common, it has been observed in several studies (*24*, *28*), though underlying biological phenomena in relation to structural growth either were noted but not resolved (*28*) or ignored (*24*).

Lacking cellular level information of the sampled trees' xylem production dynamics, processes underlying the late-summer (Fall) shrinkage (expansion) phases can, at best, be inferred from relevant existing studies. Previous work that observed rewet expansion hypothesized that rapid Fall circumference increases above previous maximums could be related to "inflation" of xylem elements whose expansive phases had been inhibited by low plant water potential during a preceding period of drought (*28*). Such latent growth (i.e. partially developed xylem element accumulation) over the previous extended period (week to month scale) is unlikely given other studies which suggest that expansion-inhibiting conditions do not delay individual tracheid development but instead lead to malformation (*40*, *41*); therefore, severe water potentials do not appear to halt initiated element development, but instead affect mature cell anatomy. Related xylem changes would be reflected in cell dimensions and wood density; such changes would not contribute to significant latent development that could become rapidly visible months later as many cohorts of cells

simultaneously resume expansion. Lempereur, *et al.* (2014) temper the latent growth hypothesis with the admission that fall rewet magnitude is related to the magnitude of primary growing season growth. In their work, trees with no detectable early-season growth do not exceed their initial circumference when they expand from summer minimum upon Fall rewet. Other indirect evidence that rapid circumference upon Fall rehydration is not indicative of proximate xylem growth is that nearly all extra-tropical forests display single growth periods per year; exceptions have been found in locations in which winter temperatures are on average above freezing (*42*). From an adaptive point of view, initiation of a second period of xylem development during the Fall would threaten functional loss of incompletely developed xylem elements; this is because complete xylem development requires weeks to months (*31*, *43*). Fall-initiated xylem development therefore extend into sub-freezing periods.

An alternative to sudden structural growth in the Fall is that both summer shrinkage and fall rewet expansion are related predominantly to hydration changes external to the xylem. In most previously studied conifer systems, daily bole expansion and contraction in relation to transpiration and shifting internal water potentials has been linked primarily to volume changes in the elastic phloem tissues (*20*). Multi-day periods of circumference decrease have been associated with high demand/low supply moisture conditions which prevent full recharge of internal water stores during the nighttime. This matches the summer shrinkage period observed at the UIEF monitoring site. However, it has also been posited that low xylem pressure during daytime or multi-day shrinkage periods prevent the expansive phase of xylem development; development would therefore be limited primarily to the nighttime or well hydrated conditions (*20*). The apparent latent increase in woody volume found at the study site between summer maximum and Fall rewet (and through the following year) indicates otherwise; either growth before the summer maximum was consistently underestimated due to simultaneous continuous shrinkage of tissues external to the xylem or structural growth continued into the shrinkage period. In the methods of the following Chapter 3, it was assumed that all woody structural growth in a given year was achieved by the summer maximum circumference and that "missing" growth, as measured following post-summer expansion, was due to underestimation during the visible growing season. It is reasonable that the mid-summer conditions of this region---consisting of high evaporative demand and multiple months at wilting point soil moisture—would be likely to inhibit xylem

growth; cambial division and xylem expansion are commonly thought to be more sensitive to extreme physical variables (e.g. water potential) than processes such as photosynthesis (*41*). Furthermore, studies on regional Douglas fir have demonstrated that northern Rocky Mountain seed sources have dramatically shorter growing seasons than coastal varieties and that structural growth cessation by August is realistic (*34*, *44*). Ultimately, because the band dendrometers employed here record circumference signals integrated from tissues including and external to the xylem, conclusive resolution of the latent growth dynamics inferred here would require intra-seasonal studies of cellular dynamics (*31*, *43*).

Degree of circumference variation at a daily and greater scale varied considerably between site species. In both 2015 and 2016, early season rain was associated with sequential periods of rapid expansion and low growth or shrinkage. These non-diurnal variations were particularly pronounced in Western redcedar when compared to Douglas fir and Grand fir. Western larch was excluded from analysis specifically because apparent rain-related variations overcame the growth signal in what were found to be exceptionally poorly performing individuals. Western redcedar consistently displayed short term variations that both significantly exceeded and underperformed longer-term (10 day) smoothed traces (Figures 2.12 & 2.13). As a species, cedar also demonstrated relatively low proportions of individuals exhibiting growth during each day of the growing season, particularly following the cessation of the rainy period (Figure 2.11). Within-species variation of cedar trees in 2015 was strongly related to variation in growth rate, driven by high individual variation during rapid growth events. Both Douglas fir and Grand fir demonstrated summer period fluctuations that were proportionately smaller than Western redcedar. In contrast to Western redcedar, Douglas fir demonstrated winter expansion that was less compensated for by spring shrinkage; therefore, though cedar exhibits heterogeneous growing season circumference, cedar rewet circumference is more consistent with the “final” yearly circumference measured the next spring compared to Douglas fir. Douglas fir is known as a more xeric species than Western redcedar and may therefore exhaust xylem water stores (and experience more costly embolism of tracheids, as well as wood shrinkage) more than western redcedar; previous work on Douglas fir has demonstrated that Douglas fir sapwood serves as a storage reservoir for water available to daily transpiration and that sapwood relative water content reaches a

yearly low by the beginning of August, with complete recharge not occurring until the early winter months of the following year (*45–47*).

The greater intra-seasonal variation of Western redcedar than other species has several non-exclusive explanations. To begin, the multi-day periods of circumference shrinkage displayed particularly by cedar trees demonstrated that the band dendrometers were not recording woody growth only. While the results of this study force us to examine hydration-related causes of a noise-filled (and sometimes dominated) growth signal, it seems prudent to not take all extra-diurnal variations (even positive) as indicative of xylem formation, even in less extreme conditions. Here, Western redcedar circumference fluctuation is likely the result of phloem and/or external bark swelling and shrinking in response to changing hydration. Greater phloem variations, and therefore water storage variations, have several possible causes, including tissue structural properties (phloem modulus of elasticity, phloem thickness, inter-tissue connectivity) and plant physiology (plant mediated phloem osmotic potential and xylem water potential) (*20*).

Prevalent hydration-related changes to outer bark thickness are supported by circumstantial evidence *in situ* and in lab experiments on stem segments. One automated dendrometer was installed on a large dead Western larch at the study site; the tree expanded and contracted by > 5 mm on a seasonal basis. The variation consisted of expansion from fall rewet through spring snow melt, after which drying-related shrinkage commenced. The patterns of this single stem were closely matched by those of several live but poorly performing larches; wood cores confirmed that those live larches exhibited negligible growth (<0.1mm), rendering their circumference variations indicative of the degree of non-growth variation (for our purposes: noise). These seasonal patterns partially match the winter expansion/spring shrinkage seen in Western redcedar, and, to a lesser extent, Douglas fir and Grand fir. The magnitudes of the seasonal patterns are consistent with outer bark characteristics; Douglas fir and Grand fir barks are denser than Western larch and Western redcedar barks, which are respectively corky and fibrous and can become water-logged. In an indoors wetting experiment performed on stem segments from Douglas fir and Western redcedar, wetting resulted in circumference increases that were difficult to detect in Douglas fir and were as extreme as the millimeter scale for Western redcedar.

While stem shrinkage is inconsistent with growth-only signals, severe positive circumference events are also likely unrelated to an actual xylem signal. Fall rewet maximum and average expansion rates greatly exceeded normal growth rates during the favorable, pre-drought portion of the primary growing season. In the Fall, comparatively cool temperatures, low incident radiation, and preceding drought stress make exceptional xylem formation rates unlikely (*31*, *48*). Furthermore, drastically altered xylogenesis would likely leave a distinct footprints in wood densities that were not found in core samples of this study (*42*, *49*). Within the main growing season (spring through mid-Summer), comparatively rapid expansion rates, as displayed in Western redcedar, are less obviously unrelated to growth. However, the apparent obligate association of rapid expansion rates with subsequent shrinkage events (Figure 2.12) strongly suggested that rain events led to exceptional noise---likely a non-xylem hydration that was erased as the environment dried over the following days. Short of complex mechanistic modeling and a cohort of continuous auxiliary measurements, studies in relatively well-hydrated forests have dealt with mid-term hydration fluctuations by creating smoothed plots from local maximums (*50–52*). This technique relies on relatively frequent and consistently dispersed low water stress conditions which are not typically found during the study region's summers; the UIEF site, following a short period in the early growing season, is instead characterized by consistent depletion of soil moisture combined with intensification of evaporative demand through the late summer. An underlying "fully hydrated" or "fully depleted" plant status is therefore unable to be assumed to be apparent at points across the entire growing season.

Automated dendrometer estimates of species-level growth metrics were characterized by relatively high variation in combination with low sample sizes. Power analyses (not reported here) generally suggested that detection of mean differences of the size suggested in the above results would require species sample sizes of several dozen. The 100 manual dendrometers measured during 2016 were able to detect such differences; furthermore, analysis indicated strong agreement between paired automated and manual dendrometers. Reasonable agreement was also demonstrated between both varieties of dendrometer and tree cores. Both automated dendrometer bands and core radial increment indicated that woody growth was greater in 2015 than 2016. The ability of automated dendrometer-derived woody growth to closely approximate inter-annual growth variation

found in cores would represent an important step in improving growth estimations; while wood cores may demonstrate inter-annual growth differences within a given radial file, automated dendrometers integrate growth around the entire bole circumference, potentially yielding more accurate absolute estimates of growth.

Comparison of automated dendrometer data between years did not demonstrate differences in growth magnitude, though larger sampled measures from wood cores and manual dendrometers indicated a modest decrease in growth from 2015 to 2016. This mild decrease along with the inability of dendrometers to detect any significant differences is surprising given the extreme drought of 2015, which we hypothesized would greatly inhibit woody growth in relation to more typical growing seasons (*41*, *53*). Automated dendrometer data did demonstrate longer growing seasons (earlier/later start/end dates) during 2016, although, with similar magnitudes of growth, this was manifested as lower growth rates. Furthermore, without validation from an isolated woody growth signal, accurate growing season boundaries may be difficult to detect; for instance, the July 2015 maximum summer circumference date found across many Western redcedars coincided with a brief rain event followed by shrinkage until Fall rewet. Similarly, initiation of growth in 2015 coincided with a significant rain event after an unseasonably dry early Spring. These events may have no causal relationship, hydration related changes may have masked growth boundaries, or locally exceptional hydration could play a role in xylogenesis initiation (*54*, *55*). Among other possible environmental drivers, snowmelt and soil warming began earlier in 2015 than 2016; 2015 did experience sporadic-sub freezing daily minimums a few weeks later than 2015, though temperatures otherwise rose earlier and at a more rapid rate, which previous research indicates should lead to earlier cambial growth initiation (*56*). Examining the influences of environmental variable thresholds on the initiation of spring circumference growth could be better resolved with further years of site study with which to compare singular yearly environmental and tree phenological thresholds.

Given the signal complexity detailed above, theoretically-justifiable extraction of intra-seasonal growth signals requires several basic assumptions and smoothing of circumference patterns at more than a daily scale. In Chapter 3 woody volume and mass growth estimation is approached with such a smoothing protocol.

Figures

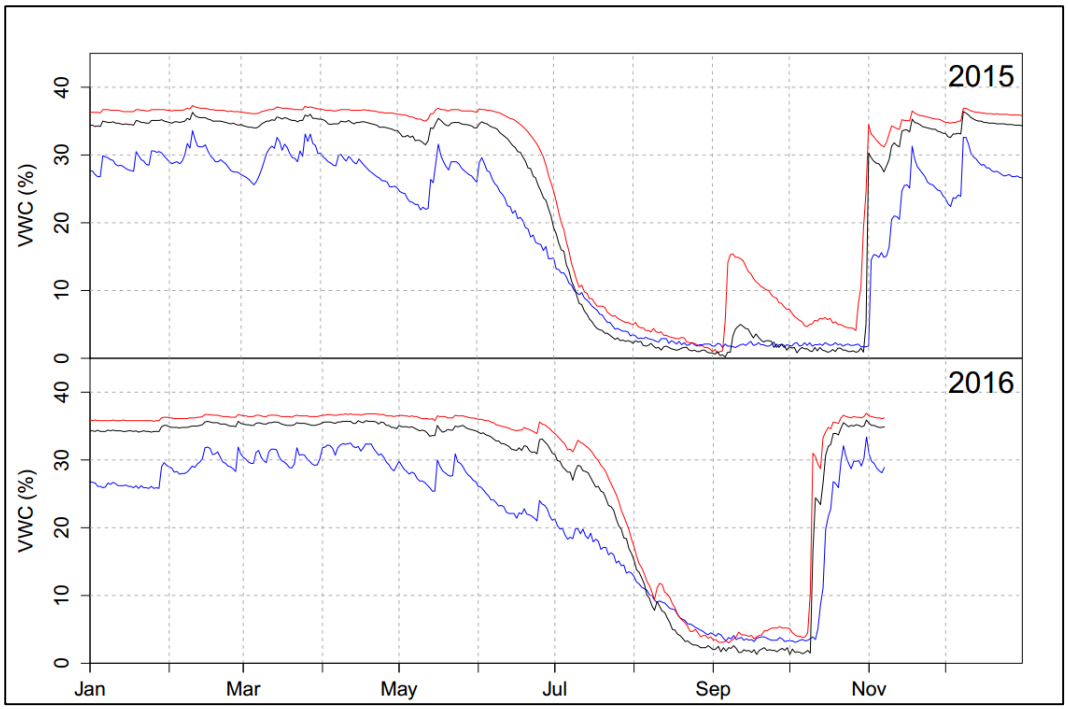

Figure 2.1. Moscow Mountain Snotel soil Volumetric Water Content (%), 2015 (A) & 2016 (B). Red line=2cm, Black line=8cm, Blue line=20cm.

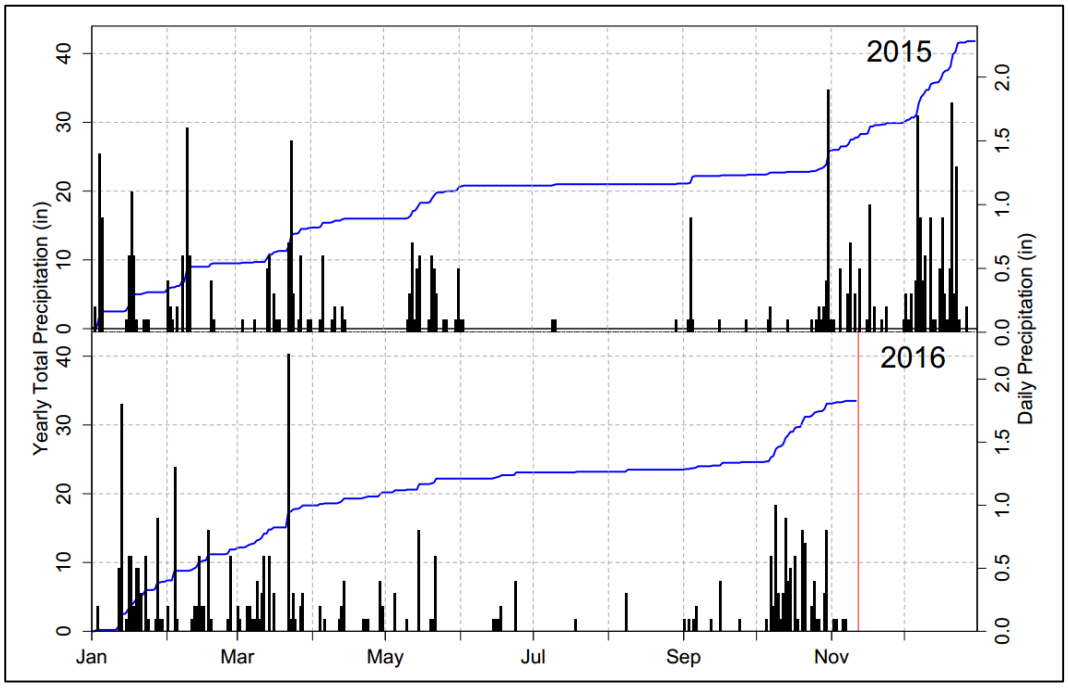

Figure 2.2. Moscow Mountain Snotel Yearly Accumulated and Daily Precipitation, 2015 & 2016. Black bars=Daily precipitation, Blue line=Yearly total precipitation.

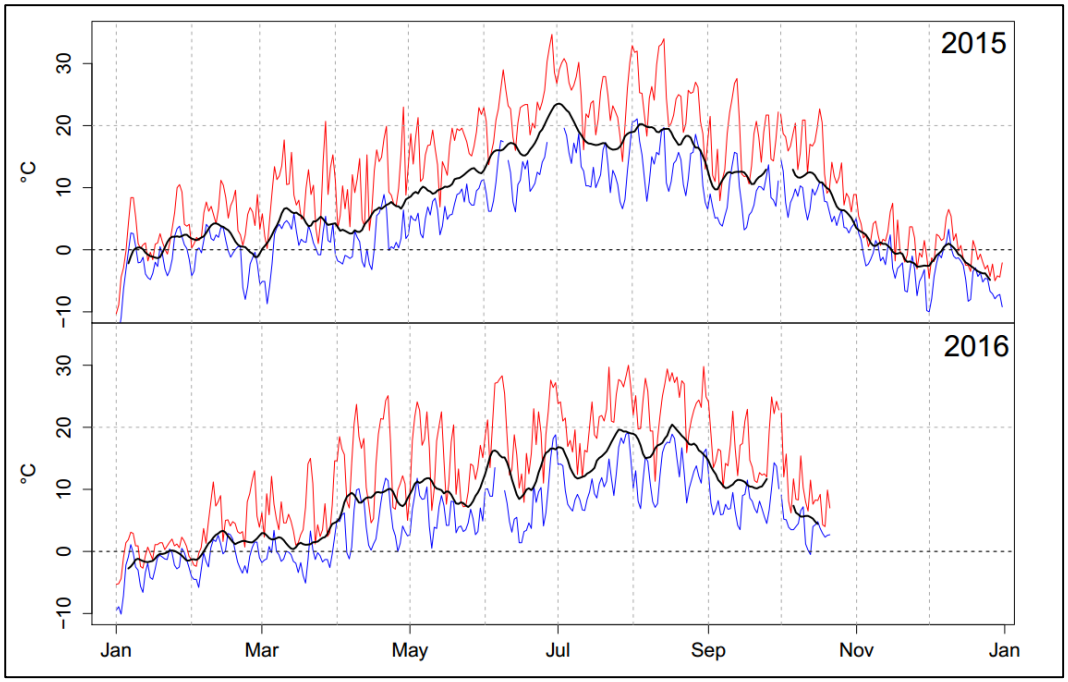

Figure 2.3. Moscow Mountain Snotel Daily Air Temperature. Red line=Daily Max, Blue line=Daily Min, Black line = 5-day daily average moving average.

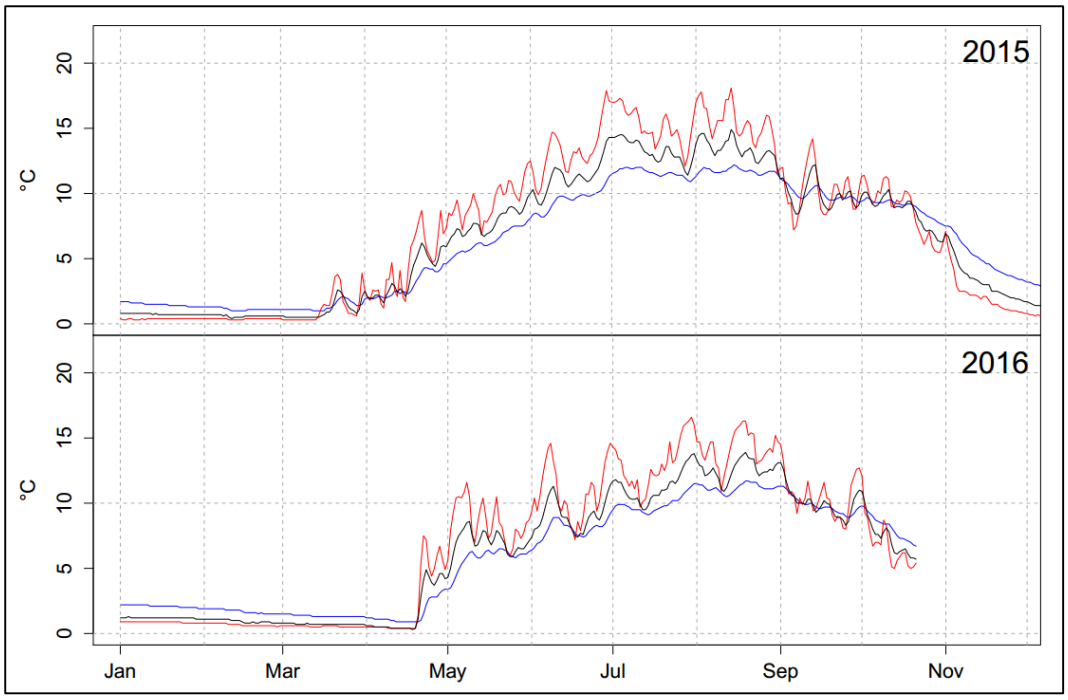

Figure 2.4. Moscow Mountain Snotel Soil Temperature. Red line=2cm, Black line=8cm, Blue line=20cm.

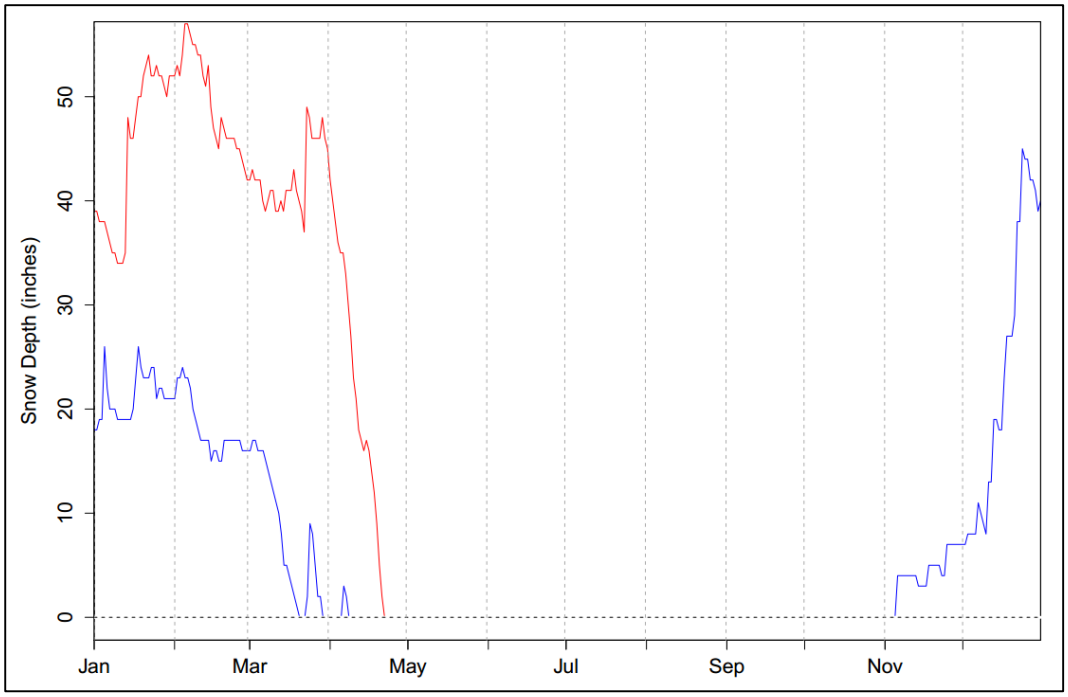

Figure 2.5. Moscow Mountain Snotel Snow Depth. Blue line=2015, Red line=2016.

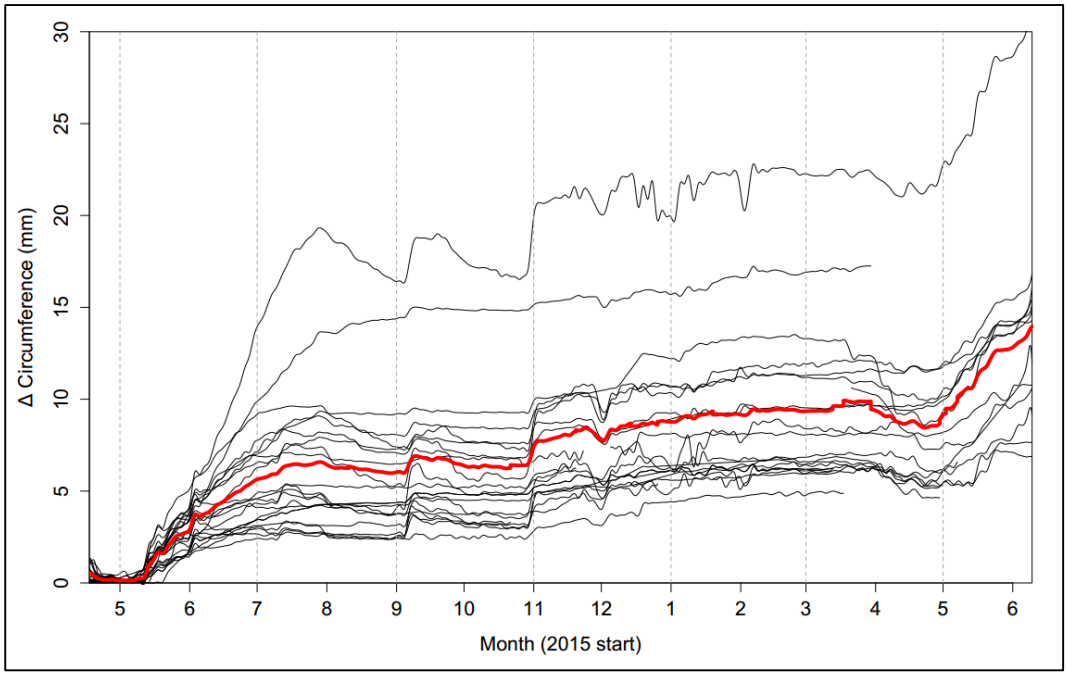

Figure 2.6. 2015 automated dendrometer Δ Circumference (Total Growth). Black lines= individual tree traces, Red line= mean

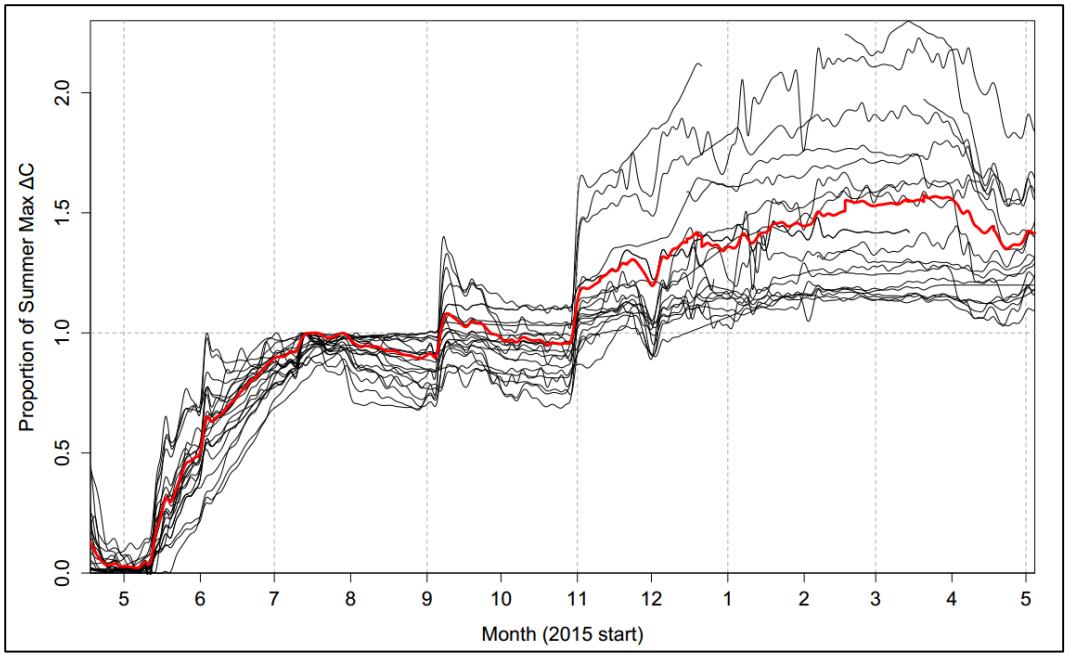

Figure 2.7. 2015 automated dendrometer normalized Δ Circumference. Each trace is normalized to summer maximum circumference (1.0=summer maximum). Black lines=individual tree traces, Red line=mean.

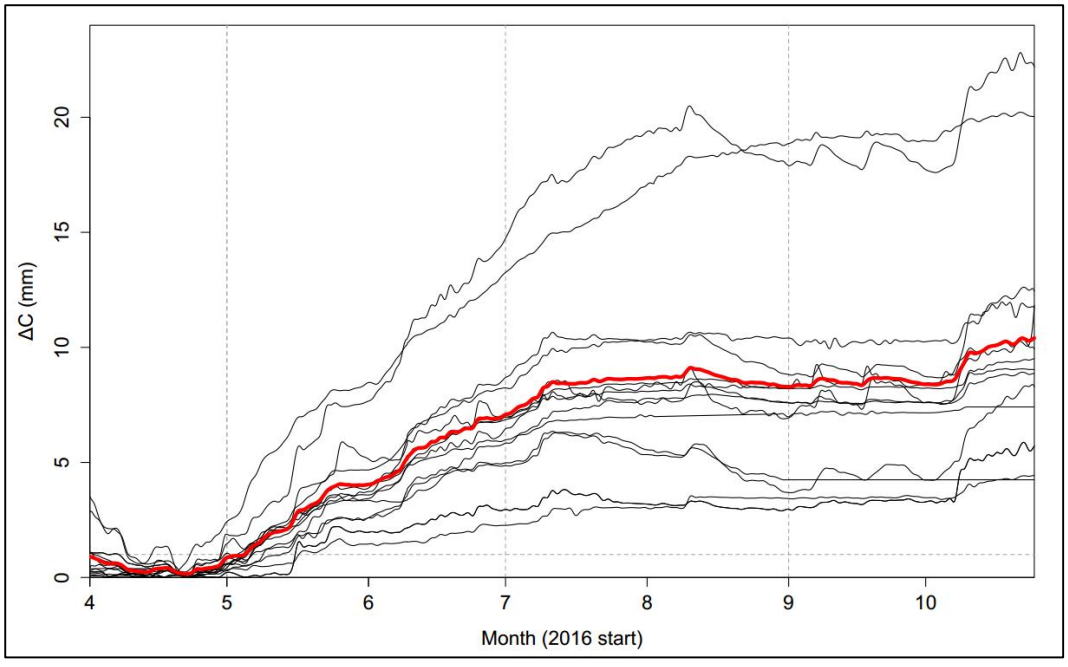

Figure 2.8. 2016 automated dendrometer Δ Circumference (Total Growth). Black lines= individual tree traces, Red line= mean

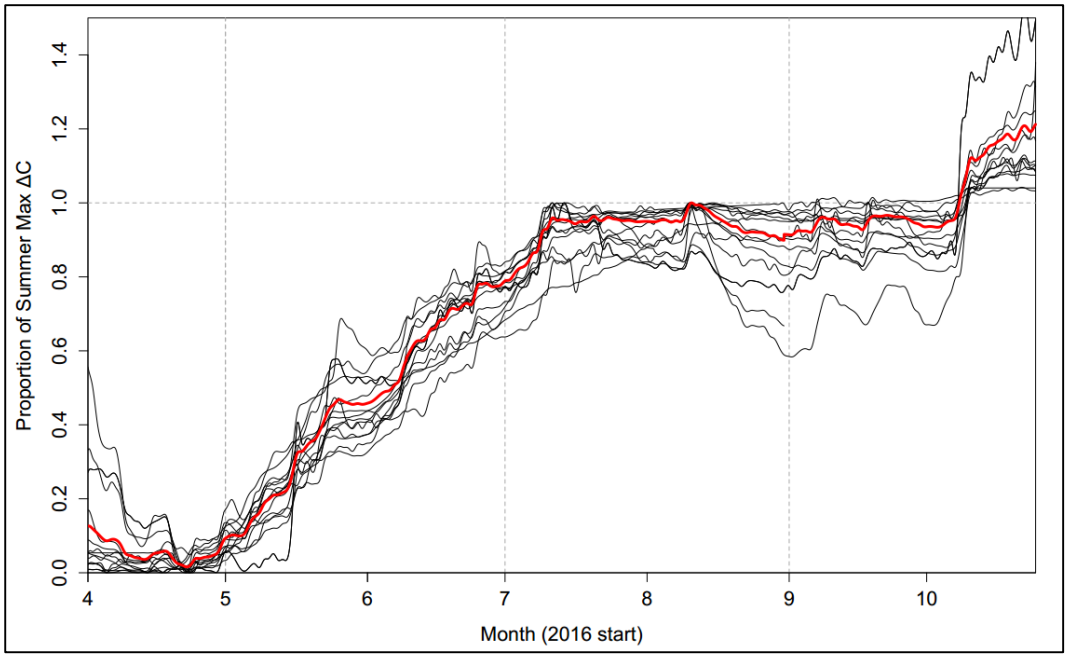

Figure 2.9. 2016 automated dendrometer normalized Δ Circumference. Each trace is normalized to summer maximum circumference (1.0=summer maximum). Black lines=individual tree traces, Red line=mean.

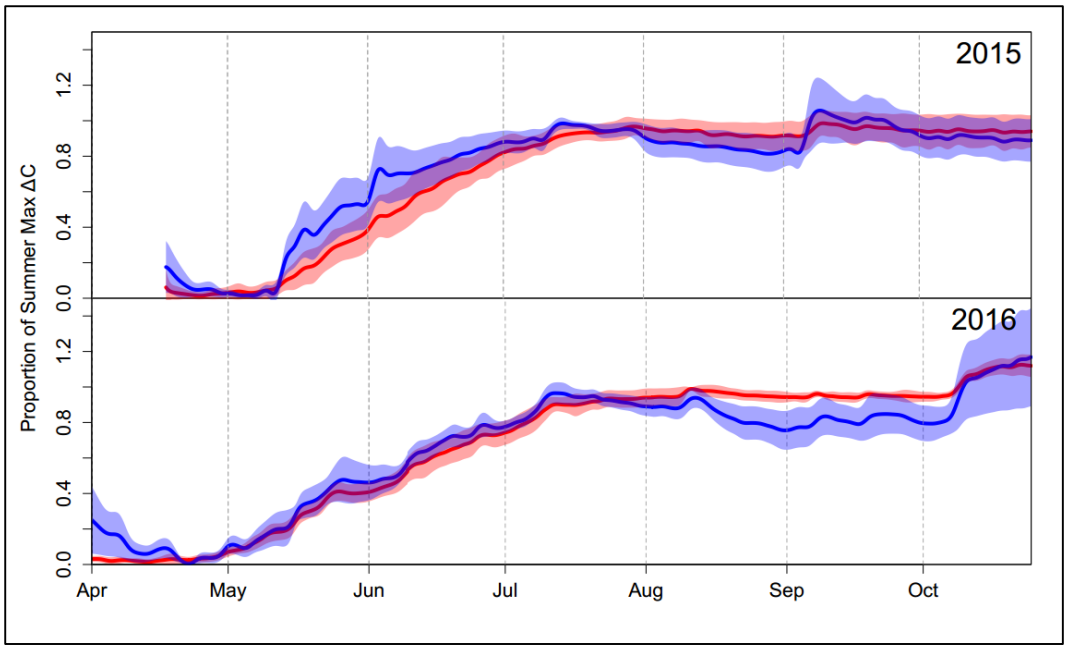

Figure 2.10. Species average normalized Δ Circumference, 2015 & 2016. Red lines=Douglas Fir mean, Red shading=Douglas fir mean ±SD, Blue lines=Western redcedar, Blue shading=Western redcedar mean±SD.

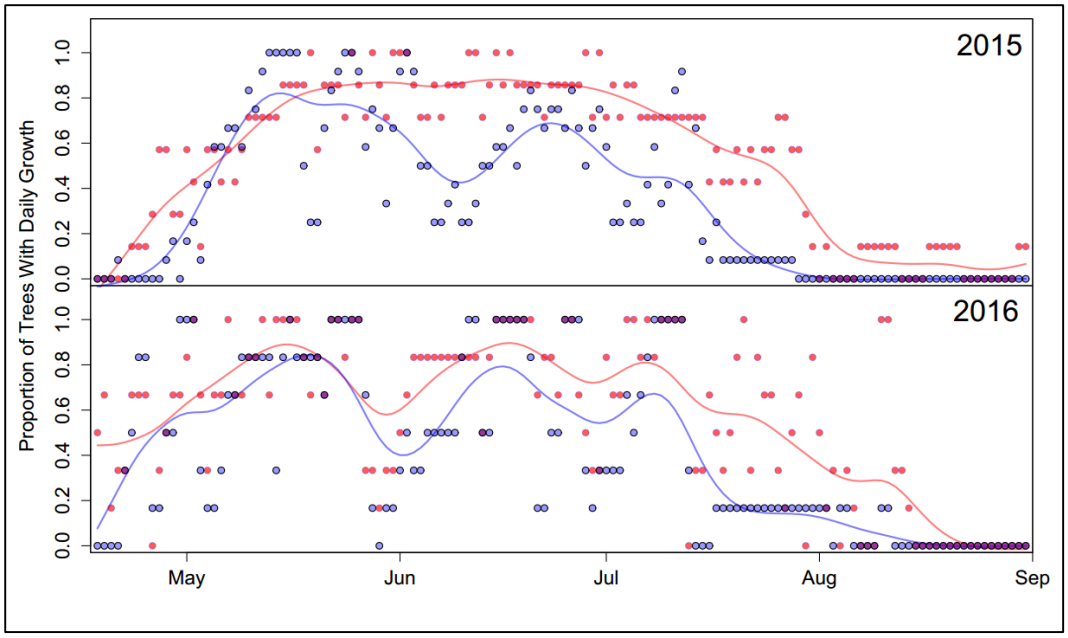

Figure 2.11. Proportion of species individuals exhibiting growth per day, 2015 & 2016. Red points=Douglas fir proportion, Red line=Douglas fir 10-day smoothing spline proportion, Blue points=Western redcedar proportion, Blue lines=Western redcedar 10-day smoothing spline proportion.

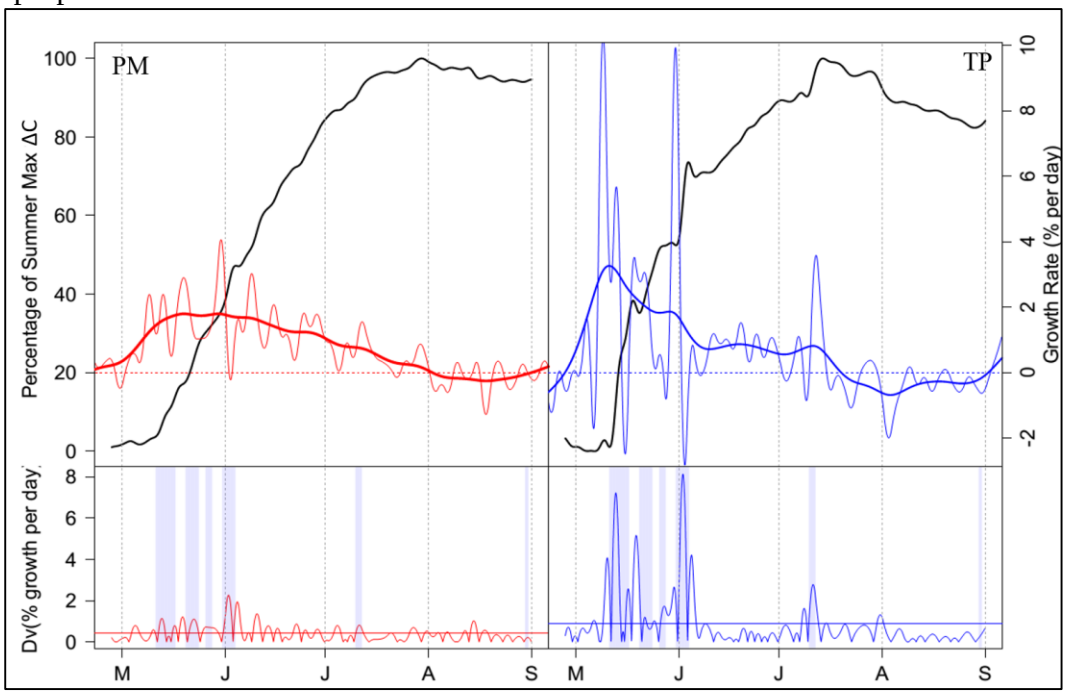

Figure 2.12. 2015 Growth rates and short-term deviations. A & C = Douglas fir (red lines), B & D = Western redcedar (blue lines). A & B show normalized average total Δ Circumference (black lines); daily Δ Circumference rates (thin colored lines) and 10-day smooth spline daily Δ Circumference rates (thick colored lines). Rates are presented as percent of summer maximum circumference per day. C& B show deviations between daily and 10 day rates from A & B. Horizontal bars indicate growing period means (pre summer shrinkage). Blue shading denotes daily rain events.

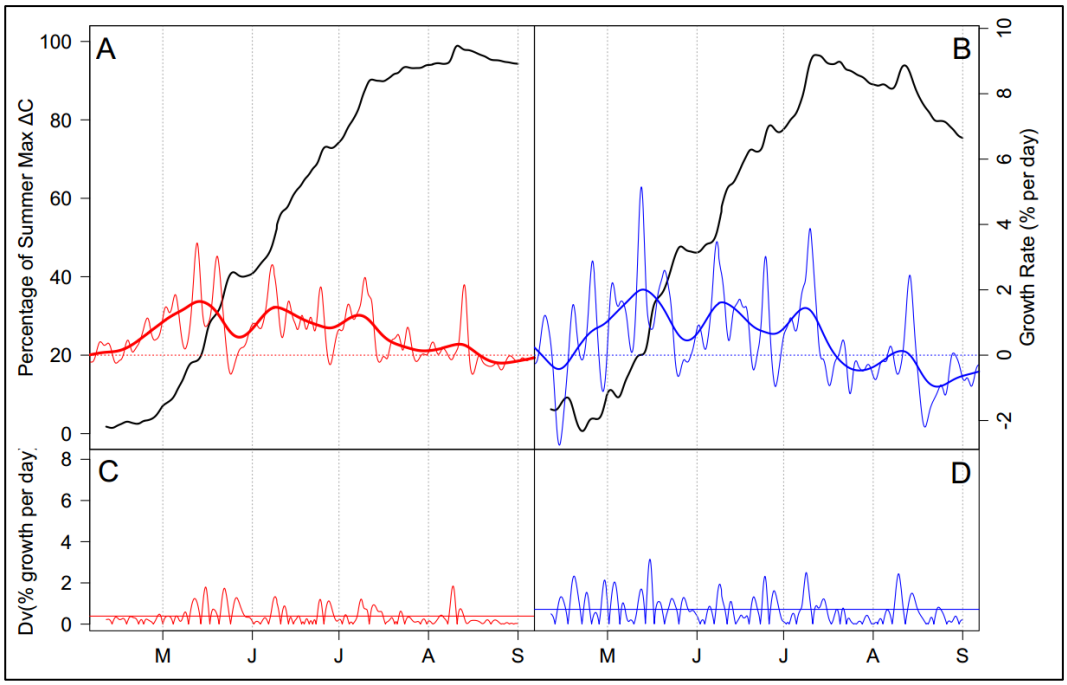

Figure 2.13. 2016 Growth rates and short-term deviations. A & C = Douglas fir (red lines), B & D = Western redcedar (blue lines). A & B show normalized average total Δ Circumference (black lines); daily Δ Circumference rates (thin colored lines) and 10-day smooth spline daily Δ Circumference rates (thick colored lines). Rates are presented as percent of summer maximum circumference per day. C& B show deviations between daily and 10 day rates from A & B. Horizontal bars indicate growing period means (pre summer shrinkage).

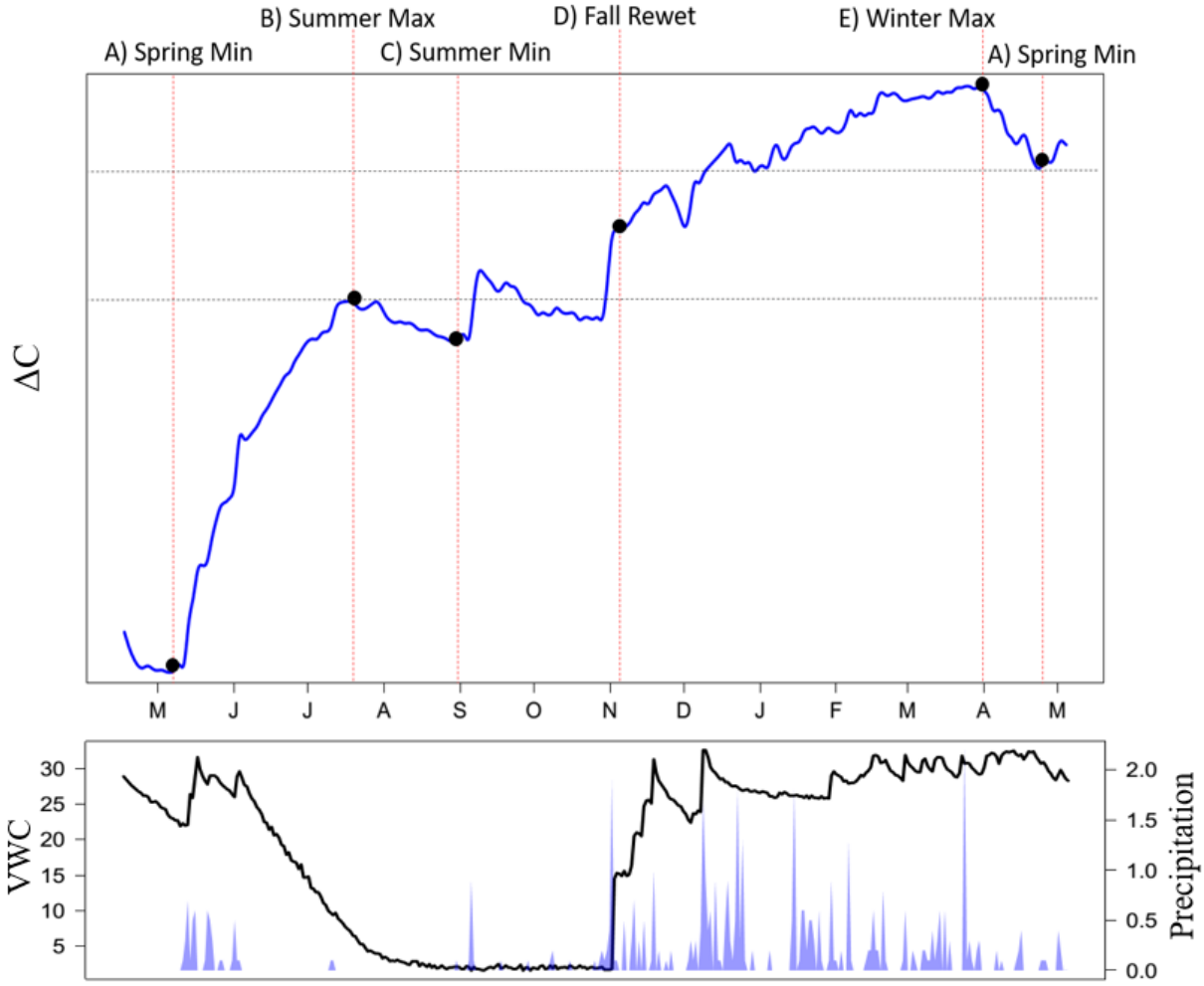

Fig 2.14. Top: Conceptual diagram of circumference variation (ΔC) and stage boundaries across one year. Bottom: Environmental variables associated with seasonal drought; Black line= Volumetric Water Content (VWC) at 20cm depth; Blue shading=daily precipitation. Data from Moscow Mountain Snotel station, 2015.

Table 1. 2015 Circumference Variation Measures. Metrics with (T) notation indicate yearly total ΔC to that time. Other metrics represent differences/proportions of compared total values. P-values are derived from two-sample t-tests with Douglas fir and Western redcedar trees.

Variation Magnitude (mm)	*Abgr (n=2)*	*Psme (n=7)*	*Thpl (n=12)*	*All Spp (n=21)*	*p-value*
Summer Max (T)	4.43	8.07 (3.69)	6.43 (4.55)	6.79 (4.08)	0.40
Rewet (T)	4.59	8.53 (3.92)	8.17 (5.44)	7.90 (4.51)	0.88
Winter Max (T)	6.34	10.19 (3.86)	9.81 (4.86)	9.76 (4.34)	0.85
Spring Min (T)	5.72	8.78 (2.76)	8.04 (4.65)	8.16 (3.92)	0.69
Summer Deficit	0.40	0.63 (0.57)	1.32 (0.98)	0.99 (0.87)	0.08
Rewet - Summer Max	0.16	0.46 (0.41)	1.14 (0.61)	0.74 (0.68)	0.03*
Spring Min - Summer Max	1.23	1.75 (0.49)	1.47 (.82)	1.55 (0.70)	0.38
Winter Max - Rewet	2.50	1.66 (0.45)	2.40 (1.29)	2.08 (1.01)	0.16
Spring Min- Rewet	1.89	1.37 (0.50)	0.21 (0.67)	0.78 (0.85)	<0.01*
Spring Min - Winter Max	-0.61	-0.29 (0.45)	-1.77 (1.30)	-1.21 (1.26)	<0.05 *
Variation Proportion (A / B)	*Abgr (n=2)*	*Psme (n=7)*	*Thpl (n=12)*	*All Spp (n=21)*	*p-value*
Summer Max, Rewet	*0.99*	*0.95 (0.05)*	*0.81 (0.14)*	*0.89 (0.14)*	*0.03**
Summer Max, Spring min	0.79	0.78 (0.10)	0.78 (0.15)	0.78	0.95
Rewet, Winter Max	0.61	0.81 (0.11)	0.75 (0.12)	0.77 (0.12)	0.32
Rewet, Spring Min	0.67	0.82 (0.11)	0.97 (0.11)	0.89 (0.14)	0.02*
Winter Max, Spring Min	0.90	0.96 (0.06)	0.81 (0.11)	0.86 (0.12)	<0.01*

Table 2. 2016 Circumference Variation Measures. Metrics with (T) notation indicate yearly total ΔC to that time. Other metrics represent differences/proportions of compared total values. P-values are derived from two-sample t-tests with Douglas fir and Western redcedar trees.

Variation Magnitude (mm)	*Abgr (n=2)*	*Psme (n=6)*	*Thpl (n=6)*	*All Spp (n=14)*	*p-value*
Summer Max (T)	13.24	8.06 (2.40)	9.37 (5.92)	9.37 (4.96)	0.63
Rewet (T)	13.68	8.59 (2.42)	10.79 (6.39)	10.22 (5.10	0.50
Summer Deficit	0.30	0.61 (0.31)	2.04 (0.70)	1.18 (0.91)	<.01*
Rewet - Summer Max	0.41	0.53 (0.15)	0.82 (0.42)	0.62 (0.32)	0.20
Variation Proportion (A / B)	*Abgr (n=2)*	*Psme (n=6)*	*Thpl (n=6)*	*All Spp (n=14)*	*p-value*
Summer Max, Rewet	0.97	0.93 (0.03)	0.90 (0.10)	0.93 (0.06)	0.51

Chapter 3: Woody NPP characterization

Methods

Density Measurement and Estimation: X-ray density profiles of six wood sections (3 each from Douglas fir and Western redcedar trees felled on site in 2016) were acquired with using a QTRS-01X Density profiler (Quintek Measurement Systems). Dried sample sections were cut to a thickness of 1.3mm. Measurements were performed at 0.04mm steps and profiles were parameterized with measured densities of samples (from mass and volume). To extend density estimates to automated dendrometer trees on which wood cores had been taken, the species-specific relationships between X-ray density and Blue Light Intensity were examined. Leveraging blue light density as a pseudo-density proxy has recently been explored in the field of dendrochronology due to the relative ease of data collection compared to time and equipment intensive x-ray techniques (*57–59*). The Blue Intensity technique involves extracting the blue channel from high-resolution scanned images, which has been found to maximize correlation with wood density. While consistency across years due to color-altering extractives and across research groups due to scanner conditions has been a concern for researchers looking to consistently estimate tree-climate proxies across many years, changes to wood color within the most recent year or several years of sapwood-only profiles was a minimal concern within this study. Wood cores were mounted with the transverse plane remaining visible (tracheid cross-sections visible) and sanded with progressively finer sandpaper through 1500 grit. Full color scanned images of sanded wood cores were taken at 2400 dpi on an Epson Perfection V800 scanner. With this resolution and sample preparation, individual tracheids were discernable in scanned images. ImageJ software (*60*) was utilized for blue channel extraction and export of resulting gray-scale value profiles. Scanned core sections from which profiles were extracted were rotated to provide measurements parallel to radial cell series. In this study, comparisons of wood section x-ray density values to Blue light intensity values demonstrated robust pattern matches, with R-squared values consistently greater than 0.98. Both Western Redcedar and Douglas fir yearly increments demonstrated consistent minimum, maximum, and mean densities. Independent calculations of transformed Blue Intensity density profile based on measured average species' density ranges produced

mean bulk increment densities that were within one standard deviation of x-ray technique mean. As a result, Blue light density profiles for cores from automated dendrometer trees were transformed using species-specific minimum and maximum density parameters and a resulting constant within-season range.

Wood Volume Growth Estimation: The first section highlights the large short term and seasonal fluctuations precluding precise evaluation of woody circumference growth at a daily scale, especially in Western redcedar and in relation to precipitation events. Without the biometric and physiological measurements necessary to directly evaluate or model woody growth, seasonal growth was therefore estimated by fit of Gompertz functions to each individual circumference trace for 2015 (Figure 3.7; R base: "nls()"); The function employed follows the form:

$$\Delta C = ae^{-be^{-ct}}$$

ΔC represents total yearly circumference growth in relation to elapsed time. Coefficient *a* represents the function asymptote, *b* sets the x-axis offset, and *c* defines the rate of growth. Gompertz curves are sigmoid functions that allow for more gradual cessation than initiation of growth and have previously been employed to estimate xylem development underlying fluctuating dendrometer signals (*30*, *36*, *48*, *61*). In some studies, Gompertz functions have been fit to only maximum values per fixed period of time; the logic of this filter is that maximum values per period represent well-hydrated extra-xylem base conditions against which to extract predominant growth signals. Functions in this work were fit against all 2015 values from the beginning of 2015 measurements (April 17th) through September 1st due to inferred existence of both overestimation and underestimation of underlying circumference. Local maximums in mid to late summer were not expected to represented well-hydrated conditions, while maximums during the spring were considered overestimations that likely were at least partially driven by outer bark saturation.

To manage the discrepancy between summer maximum and greater circumferences later in the year, proportional growth within the growing season was scaled by yearly total growth values that were assigned from subsequent spring minimums. Under this scheme, growing season underestimation of growth was proportional to growth rather than time. The growing season was considered to last until September 1st. The September boundary was

chosen based on it exceeding the latest dates through which the initial period of growth continued for the most persistently-growing trees observed. This date is also generally supported by cellular-level studies of regional species' xylem development dynamics (*33*).

Rates of circumference growth estimated by Gompertz fit were converted to bole volume growth via region and species-specific allometric equations (*12*).

NPP Estimation: In order to align density profiles with volume time series, mean densities for 20 equal sized cuts of each density profile were calculated. Cut means were applied to median values of 20 equally sized volume growth sections and followed by linear interpolation. Biomass growth was then estimated by multiplying individual density and volume change profiles. Tree-scale woody net primary productivity (NPP) was estimated by assuming that carbon mass was 49% of total dry wood mass (this proportion was measured in a separate mass composition analysis and was the same for both Douglas fir and Western redcedar; Grand fir average C mass proportion was 0.49).

Tree-level estimation of NPP was scaled to stand level in combination with plot inventory data, which indicated tree height, tree diameter at breast height (dbh), and species densities on a sub plot basis.

Results

Density: 2015 density profiles calculated using assumed minimum and maximum densities for stand Douglas fir (260 and 1020 kg m^{-3}) resulted in a Blue Intensity-derived mean of 555 kg m^{-3} for dendrometer tree cores, which matched well with the x-ray-technique mean of 560 kg m^{-3}. The calculated Western redcedar mean of approximately 320 kg m^{3} (min= 200; max= 805) fell below the x-ray average of 358 kg m^{-3}. This discrepancy resulted in re-finishing and re-scanning of Western redcedar cores, which demonstrated a second average yearly mean that was less than 1 kg m^{3} different. Scanned image and visible microscopy observation indicated that the 2015 seasonal progression of Blue Intensity and of tracheid diameter progression were distinct from previous years within series; many 2015 Western redcedars demonstrated relatively abrupt shifts from wide-lumen, low density early-wood (representing approximately 80% of the increment) to dense latewood, largely excluding an extended

section of mid-density transition wood (Figure 3.1). Western redcedar profiles demonstrated maximum density accelerations at 82% (+-14%) of yearly increment and doubled starting densities at 90% of yearly increment (+-4%). Average Douglas fir maximum acceleration and doubling occurred at 58% (12%) and 70% (+-23%) of yearly radial increment.

Circumference and Volume growth rates: Gompertz function-derived circumference growth rates indicated maximum rates in late May for Western redcedar and in early June for Douglas fir (Figure 3.2). On average, 5% to 95% of Western redcedar circumference growth occurred between May 5th and July 10th (67 days). On average, 5% to 95% of Douglas fir growth occurred between May 9th and July 26th (78 days). Average date of maximum circumference growth rate was May 23rd (±7 days) for Western redcedar and June 1st (±6 days) for Douglas fir (t-test, $p<.01$). The average maximum Western redcedar relative growth rate was 2.6 % of individual summer maximum ($\Delta C\ day^{-1}$) and exceeded the Douglas fir maximum average rate of 2.0% day^{-1} (also, Gompertz growth rate parameter (*c*) t-test, $p=0.06$). Both circumference growth rate profiles were positively-skewed, as dictated by the Gompertz function underlying them. Intra-species variation of growth rates among Western redcedar trees was greater than among Douglas fir, particularly during the peak growing period (Figure 3.2). For Western redcedar, monthly percentages of yearly total growth were 2.1% (±1.7%) for April, 57% (±17%) for May, 32% (±10%) for June, 7% (±6%) for July, and 1.3% (±1.5%) for August. For Douglas fir, monthly percentages of yearly total growth were 1.1% (±0.6%) for April, 38% (±12%) for May, 43% (± 6%) for June, 15% (±5%) for July, and 4% (±2%) for August.

Average R-squared values for fit Gompertz curves and dendrometer traces were 0.9945 for all individuals, 0.9977 for Douglas fir, and 0.9923 for Western Redcedar. Douglas fir R-squared values were significantly greater than Western redcedar values (t-test, $p<.01$). The Western redcedar R-squared value standard deviation (0.01) was approximately four times greater than Douglas fir value standard deviation (0.0025). Lower Western redcedar R-squared values were associated with lower summer maximum growth (ΔC); Western redcedar series with high summer maximum growth as well as all Douglas fir series demonstrated consistently high R-squared values (Figure 3.9). The average growth rate parameter ("c"; see methods description of Gompertz function) was greater for Western redcedar than Douglas fir (t-test, $p=0.06$). The mean deviation between fit growth curves and normalized circumference

profiles (April 17th through September 1st; 100%=growth through summer maximum) was 2.6%. For Western redcedar and Douglas fir, mean deviations were 3.2% and 1.8%, respectively. For both species, deviations oscillated between positive and negative through the early and mid-growing season (Figure 3.8). Western redcedar circumference measurements consistently underperformed modeled values in the late season (after early June).

Species bole volume growth profiles were offset in correspondence to circumference growth. Mean volume 2015 growth for Douglas fir was 0.014 ±0.011 m^3 (or 14,000 cm^3) and for Western redcedar was 0.010 ±0.008 m^3 (t-test, differences not significant).

NPP: Species intra-seasonal net primary productivity (NPP) displayed patterns that deviated from circumference growth rate patterns. Particularly, both Douglas fir and Western redcedar species average NPP rates demonstrated relative summer plateaus (Figure 3.3) instead of narrow rate peaks determined through Gompertz fit of circumference (Figure 3.2). Average Western redcedar retained a positive skew, while the Douglas fir skew became negative. Average calculated NPP for Western redcedar rose rapidly to a yearly maximum in the spring, declined relatively slowly through early July, and then experienced rapid decline. Douglas fir relative NPP rose less rapidly than Western redcedar NPP in the spring, reaching a relative summer plateau in June but continuing to increase through early July, after which precipitous declines occurred. The relative plateau effect seen in both species is the average of several different types of individual level NPP patterns (Figure 3.4); individual trees demonstrated narrow unimodal progressions (much like the rate patterns), widened unimodal progressions compared to rate progressions, and relative plateau patterns which typically demonstrated minor peaks. Mean peak NPP date in Western redcedar was June 1st (± 15 days); mean peak NPP date for Douglas fir was June 22nd (±11 days) (t-test, $p<.01$). This represented average circumference growth to NPP peak date shifts of +9 days for Western redcedar and +24 days for Douglas fir. Average 5%-95% NPP total occurred between May 8th and July 4th for Western redcedar (57 days) and May 15th and July 20th for Douglas fir (66 days). Average Western redcedar monthly percentages of yearly NPP were 1% (±1%) in April, 44% (±20%) in May, 38% (±10%) in June, 14% (±9%) in July, and 3% (±3%) in August. Average Douglas fir monthly percentages of yearly NPP were 0.4% (±0.4%) in April, 23% (±11%) in May, 45% (±8%) in June ,26% (±12%) July, and 6% (±5%) in August.

Across all individuals, calculated mean NPP was 2244 g C $year^{-1}$ $tree^{-1}$ (range: 564-8292 g C $year^{-1}$ $tree^{-1}$). Mean yearly Western redcedar NPP was 1465 g C $year^{-1}$ $tree^{-1}$ (range: 564-4377) while mean yearly Douglas fir NPP was 3578 g C $year^{-1}$ $tree^{-1}$ (range: 1265-8292) (t-test, p=0.09) (Figure 3.5). Growing season maximum NPP ranged between 10 g C day^{-1} and 74 g C day^{-1} for Western redcedar and 22 g C day^{-1} and 131 g C day^{-1} for Douglas fir. There was a steep positive relationship between NPP and tree size for Douglas fir (R-squared = 0.83) and a weaker, shallow positive relationship for Western redcedar (R-squared = 0.50) (see Figure 3.6 and caption).

Growth Rates and Environmental Conditions: Temperature, photoperiod, and soil moisture were key environmental variables that were examined in relation to peak woody growth. In 2015, peak temperatures were recorded from early July through mid-August (Figure 2.3). Maximum photoperiod in the northern hemisphere is in late June and in 2015 fell on June 21st. Soil moisture decline slowed in late July as wilting point soil moisture was reached. The VWC of the 20cm soil depth at the Moscow Mountain Snotel station decreased below 5% on July 24th. The Western redcedar mean NPP peak date of June 1st fell approximately one month before the hottest period of the summer and three weeks before the maximum photoperiod. The mean Douglas fir NPP peak date of June 22nd aligned closely with maximum photoperiod and decreased through the hottest portion of the summer. Both species' peaks fell before the late July exhaustion of plant available soil moisture. The Western redcedar average peak fell near the beginning of rapid seasonal soil moisture decline (occurring during the first days of June). Peak Douglas fir volume growth (June 1st) similarly coincided with the period immediately preceding rapid decline of soil moisture, while Western redcedar peak volume growth (May 23rd) occurred before this period, therefore coinciding with the period during which Spring precipitation prevented soil moisture decline.

Discussion

Calculated NPP_{wood} seasonal profiles differed markedly from the volume growth rate profiles. Aligning and then multiplying seasonal pseudo-density profiles and volume growth created estimates which displayed relative plateaus---greater-than 1 month periods when

woody biomass accumulation was calculated to be consistent relative to circumference profiles, especially at the species level (Figure 3.3). Such widening peak growth profiles are consistent with recent xylem development research (microcore-based) that has suggested that maximum biomass accumulation consistently lags maximum circumference growth and that the biomass production profile is more evenly distributed than the xylem expansion profile (*31*). Furthermore, related work has found that biomass is relatively conserved per cell, with increased durations and rates of individual cell biomass deposition balancing changes in one another; therefore, changes to duration of xylem expansion and diameter may, for the most part, necessarily lead to smaller but correspondingly denser cells (*30*, *43*).The seasonal fringes for the intra-seasonal productivity distributions of this study were methodologically constrained by when volume growth was evident, though peak shifts were clearly registered for both Douglas fir and Western redcedar. Greater seasonal peak delays for Douglas fir led to NPP profiles that peaked approximately 3 weeks later than Western redcedar. The lack of exact correspondence between volume growth and biomass growth is further expected given different controls on cell expansion versus cell wall thickening. In general, cambial growth and xylem expansion are thought to be more sensitive to ambient conditions than many other plant processes (*41*). Estimations from Cuny et al. (2015) indicate common peak volume growth to peak biomass growth lags of approximately one month in forests without severe summer drought. Similar modern microcore studies have not been performed on this study's species, though previous relevant analyses on Douglas fir indicate wall expansion and wall thickening phase phenological gaps of approximately 3 to 4 weeks (based on timing of stage initiation and cessation) (*33*). Though this study's volume growth and NPP were not calculated independently, offsets between measure peaks were consistent with the above studies stage offsets for Douglas fir (~1 month) but not for Western redcedar (~10 days). Additionally, although calculated NPP profiles displayed later and wider peaks than volume growth profiles, the calculated periods of 5% to 95% NPP were shorter than those for volume growth. One large caveat should be noted in relation to NPP calculations expressed here. Aligned volume and density were used to calculate NPP according to the time of volume growth---thus, NPP here is truly a pseudo-NPP, indicating determined, but not yet occurring productivity (i.e. dedication of carbon to tracheids still in the cell expansion stage of xylogenesis). As such, our calculations do not take into account per-cell phase lags, which can

vary from days to weeks in length (*43*). Such an accommodation could make Western redcedar Volume Growth-NPP lags more in line with literature values and would make Douglas fir lags longer.

The key, species-dependent shifts found when comparing volume growth to NPP were the result of species-dependent seasonal density progressions. On average, increasing Western redcedar densities near the end of the season were not sufficient to prevent estimated NPP decline due to their coincidence with precipitous declines in volume growth. Density increases were typically manifested as local NPP increases but did not halt the dominant rate decline. In comparison, Douglas fir density increases occurred earlier in the season and led to a more significant offset of the NPP peak. The initial volume peak was still evident as an earlier minor peak in calculated NPP. In regards to the accuracy of individual tree NPP profiles that indicated multiple minor NPP peaks---if increases in density are directly related to decreases in cell diameters and not biomass, such oscillations may simply indicate slight mismatches between volume change and density profiles. In support of this possibility, the detailed cellular-level accounting of Cuny *et al.* (2015) indicated unimodal distributions for rates of expansion and biomass deposition (*31*). Overall, however, the existence of a modifying effect of wood density on calculated NPP indicates that estimations that account for geometric change alone (with assumed average wood density) will fail to accurately assign timing of woody NPP; NPP estimations with volume growth alone can only result in NPP that is commensurate with that volume change.

Previous research has related wood developmental rates to temperature and photoperiod profiles (*31*, *48*). In this study, we found that Douglas fir peak NPP corresponded with maximum photoperiod and that peak Western redcedar NPP instead corresponded to the period preceding soil moisture decline. For this reason, it appears that Western redcedar, the most mesic site species, was more strongly constrained by moisture availability than other factors. In contrast to peak NPP, both species' volume growth rate peaks were shifted earlier in the season, supporting a greater sensitivity of expansive growth than biomass deposition to hydration. Western redcedar peak NPP and Volume growth peaks fell before periods during a significant portion of available soil moisture had been exhausted and therefore preceded what would be expected to be physiologically inhibiting soil water potentials (*41*). Therefore, peak growth in this species may be related to more to low evaporative demand and adequate

proportions of fine roots in contact with water-filled soil pores (a tree-scale soil:root conductance, not water potential, relationship). Alternatively, peak growth estimates may be overly influenced by early season hydration changes.

We approached the estimation of underlying mid-term (greater than daily and less than seasonal scale) volume and NPP progressions by fitting theoretically-justifiable general growth patterns (i.e. Gompertz functions) to integrated stem growth and hydration signals (*13, 30*). Statistical fit eliminated short term noise along with the tradeoff of accompanying elimination of any short term growth signal. However, given the lack of observations with which to differentiate the causes of those underlying fluctuations, meso-scale estimates were a necessary compromise. The methods used here demonstrated species offsets in seasonal NPP; Douglas fir, a relatively xeric species, displayed high productivity later into the seasonal drought period than Western redcedar, a mesic species. Estimated volume profiles delineated periods of seasonal expansion and allowed for reasonable estimations of when subsequent mass deposition might occur in comparison to hypothetical ecosystem model predictions. Particularly, circumference and NPP estimates displayed short primary growing periods (5% to 95%) of approximately 60 to 80 days within a much longer seasonal warm period (6-7 months). Finally, the study scaled growing season variations by yearly total growth values that were quite precise and measured in a consistent manner in comparison to traditional manual methods, which introduce measurer error; for this reason, derived seasonal patterns could be scaled by such improved biometric data and carbon flux could be more reasonably estimated.

Several essential assumptions were employed in the process of converting circumference variations to woody volume growth. The use of a Gompertz function fit for smoothing and constraining noise-filled estimates with previous research and theory is particularly appropriate if several conditions are met. First, for the fitting procedure to justifiably weigh all growing season points equally, those data points need to demonstrate no time-varying bias in regards to underlying woody volume (no long-term patterns in fit residuals deviation from actual growth) (*13*). Here, underestimation of total yearly growth during the growing season indicates that such a bias could be an issue towards the end of the visible growing season.

Another critical study assumption was that distributions of dendrometer-based growth metrics did not simply represent a range of measurement biases within or between species. For instance, dendrometer estimates of summer growth cessation were based on maximum summer circumference. Underlying individually varying relationships between displayed summer maximum circumference and total woody volume change would mean that the summary statistics employed in this study were not appropriate. In relation to this possibility, apparent circumference growth in most trees ceased before a summer shrinkage period, while growth in a few, rapidly growing Douglas fir and Grand fir individuals continued until September (see results in both sections). Two alternative explanations for this observation were that underlying wood growth timing varied between individuals or that rapidly growing/well hydrated individuals had high growth to hydration signal ratios during the late-season period of relatively low, consistent growth. The apparent earlier cessation of growth in Western redcedar than Douglas fir in this study could be explained by a greater shrinkage prior to growth cessation in Western redcedar; this was indirectly supported by high visible seasonal fluctuations in Western redcedar circumference.

Unlike increasingly affordable and low-labor automated dendrometer measurements of stem dimensional changes, the micro-core measurements necessary for fine temporal-scale density estimation (*31*, *43*, *62*) are not able to be obtained automatically. Given the lack of reasonable ease with which to measure the density component of the necessary mass flux calculation (NPP), further study is necessary to understand the degree to which intra-species density profiles vary, the extent to which such variation modifies NPP estimation, and specific classes of trees (e.g. species, vigor) that may be particularly appropriate or inappropriate for species level density parameter estimation. In this study, Western redcedar wood density deviated from measured species normals by approximately 40 kg m^3; in Douglas fir, this was not the case. In other recent work in which detailed morphometric or x-ray-derived density profiles were measured, seasonal density progressions were effectively conserved within species and across years (*43*). At the study site, more focused collection and analysis of wood profiles as well as a greater number of dendrometer circumference profiles with which to examine the effects of resulting NPP estimation would be necessary for confirmation that conserved density progressions are a reasonable assumption.

Moving forward, several strategies indicated by this pilot methodology would greatly assist in obtaining reasonably robust and inexpensive intra-seasonal NPP estimation alongside other continuously monitored carbon fluxes. Sufficient replication within the groups being examined is necessary for detection of key growth differences under an evolving climate. Evaluation of which classes of individuals may realistically provide sufficiently dominant growth signals (i.e. a high signal to noise ratio) at the desired intra-seasonal scale is also needed (*13*). From a growth perspective, this may be achieved by selecting trees that are not exceptionally slow growing. From a hydration-status perspective, this may require identifying and excluding species whose tissues are particularly elastic in their non-xylem dimensions. To partially address the issue of hydration-related circumference fluctuations, detailed preparation of trees with thick and absorptive bark is worthwhile, especially for band dendrometer installations. To better model the effects of changing hydration in tissues, point dendrometers can also be employed for auxiliary data; while currently more expensive and representative of a point, rather than circumference, on the stem, point dendrometers benefit from ease of extensive targeted bark preparation and a lack of bark-dendrometer friction affecting variation measurements. Finally, employing dendrometers alongside other flux measurements (Eddy covariance towers, soil respiration chambers, etc) will assist in evaluating and constraining growth in the context of other related tree processes.

Conclusion

This study highlights key uncertainties in the use of automated dendrometers for estimating intra-seasonal net primary productivity in the context of drought and develops a procedure for extraction of woody growth signals. Proceeding from the necessary assumptions made for calculations, results suggest relatively short growing seasons, with spring and early summer month volume growth ended by mid-summer (July to August) for most individuals. Therefore, with approximate biomass lags taken into account, underlying biomass/NPP deposition associated with that structural growth would likely be completed by September, well before the end of the period in which temperature and light conditions are favorable for plant productivity. Calculated volume, density, and NPP profiles varied between the two species that maintained reasonable dendrometer representation—Western redcedar

and Douglas fir. These profiles indicated a shorter and earlier growing season for the mesic, late successional Western redcedar in comparison to Douglas fir. The shifts between volume and NPP profiles highlight the need to scale derived volume change estimates by the several-fold increases in wood density that occur across the growing season. Such considerations reflect the reality of cell-scale biomass deposition that does not necessarily scale with individual cell dimensions. In the context of only one complete "circumference year" (designated in this study as Spring to Spring), intra-seasonal responses of profiles to intensifying drought are not able to be thoroughly examined. Future forest species responses will depend on how growth patterns change in relation to shifting optimal periods, intensifying stressful periods, and varying degrees of physiological stress. Continued measurement of study site trees as well as bolstered automated dendrometer representation are therefore necessary to provide valuable insights into the response of ecosystem net primary productivity to intensifying drought regimes.

Figures

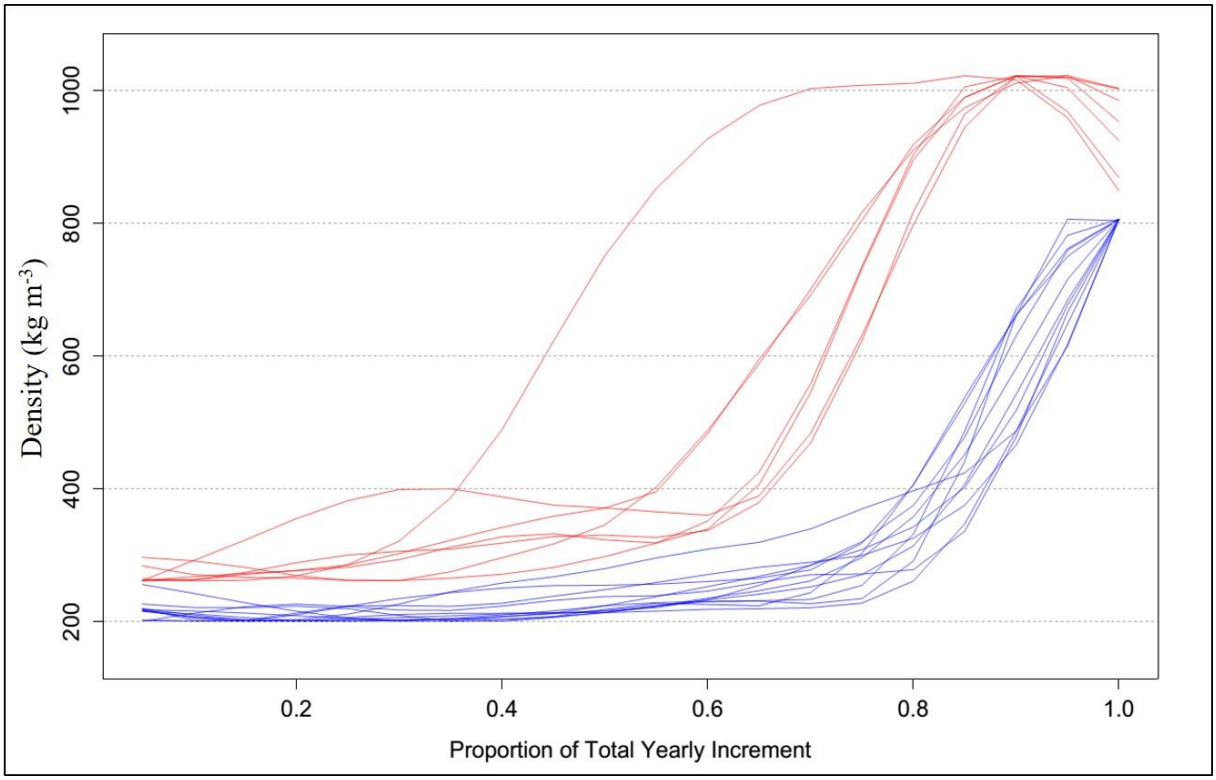

Fig 3.1. Blue Light Intensity–derived psdeudo-density profiles for individual trees [cores]. Yearly increment proportion (x-axis) progresses from the early-wood (inner core) to the late-wood (outer core). Red lines= Douglas fir; Blue lines=Western redcedar.

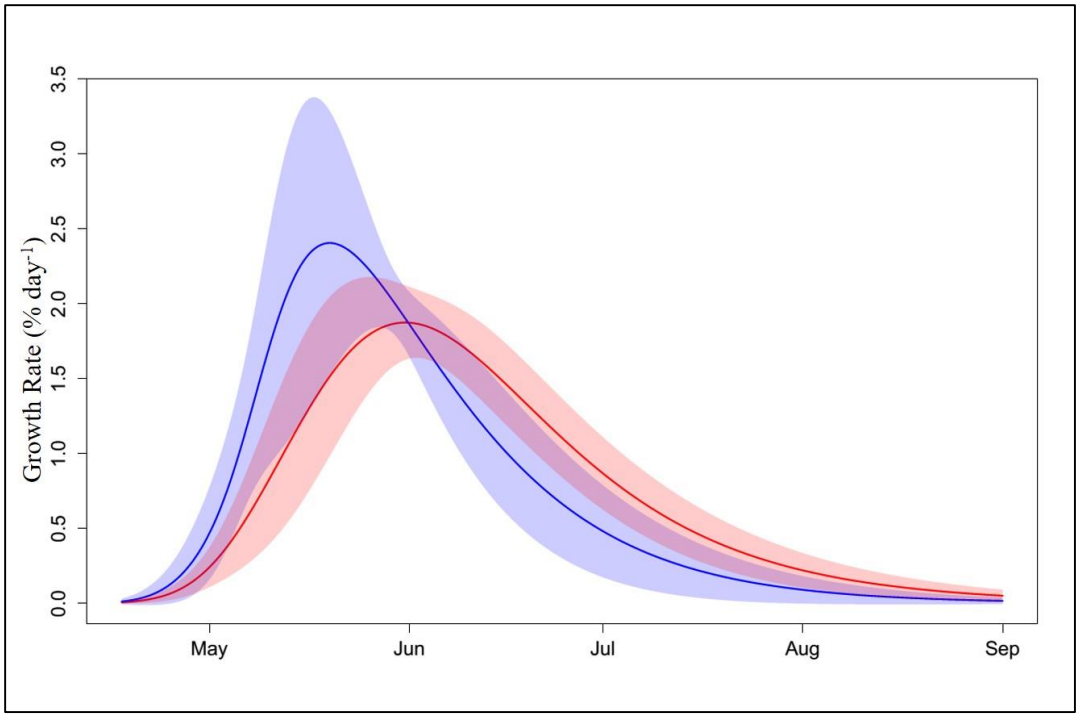

Figure 3.2. 2015 species circumference growth rate as a proportion of summer maximum. Blue line=Western redcedar mean rate; Blue shading=Western redcedar standard deviation; Red line=Douglas fir mean rate; Red shading=Douglas fir standard deviation.

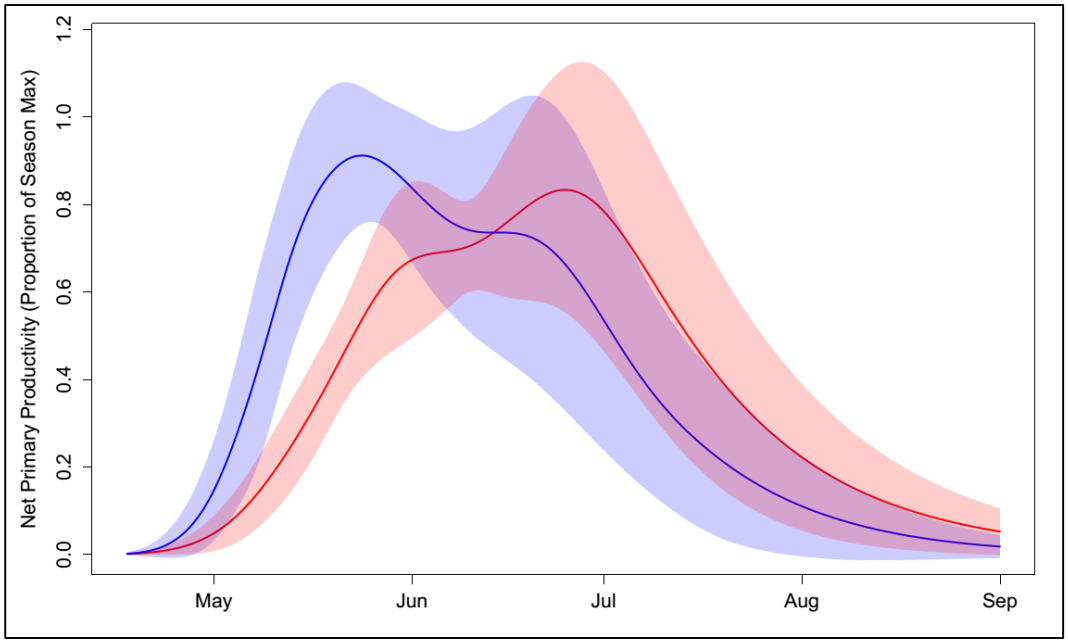

Fig 3.3. 2015 species NPP as a proportion of summer maximum NPP. Blue line=Western redcedar mean rate; Blue shading=Western redcedar standard deviation; Red line=Douglas fir mean rate; Red shading=Douglas fir standard deviation.

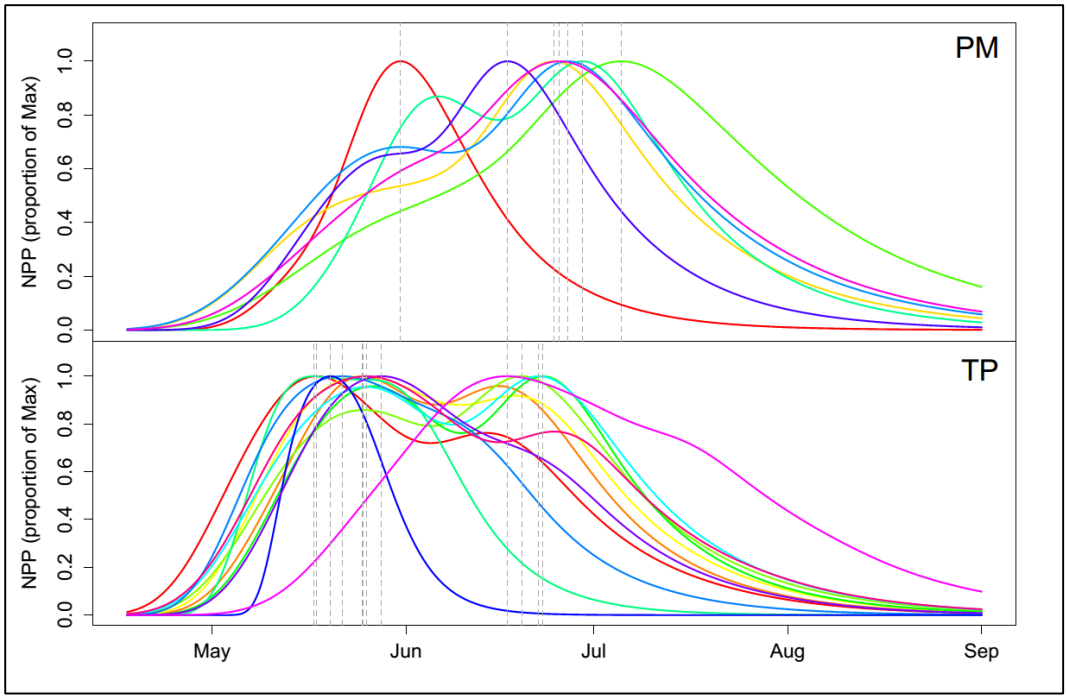

Fig 3.4. 2015 Individual tree seasonal NPP as a proportion of summer maximum NPP. Top frame (PM) = Douglas fir traces; Bottom frame (TP) = Western redcedar traces. Colors differ to visually distinguish individuals. Dotted gray lines denote summer peak NPP times.

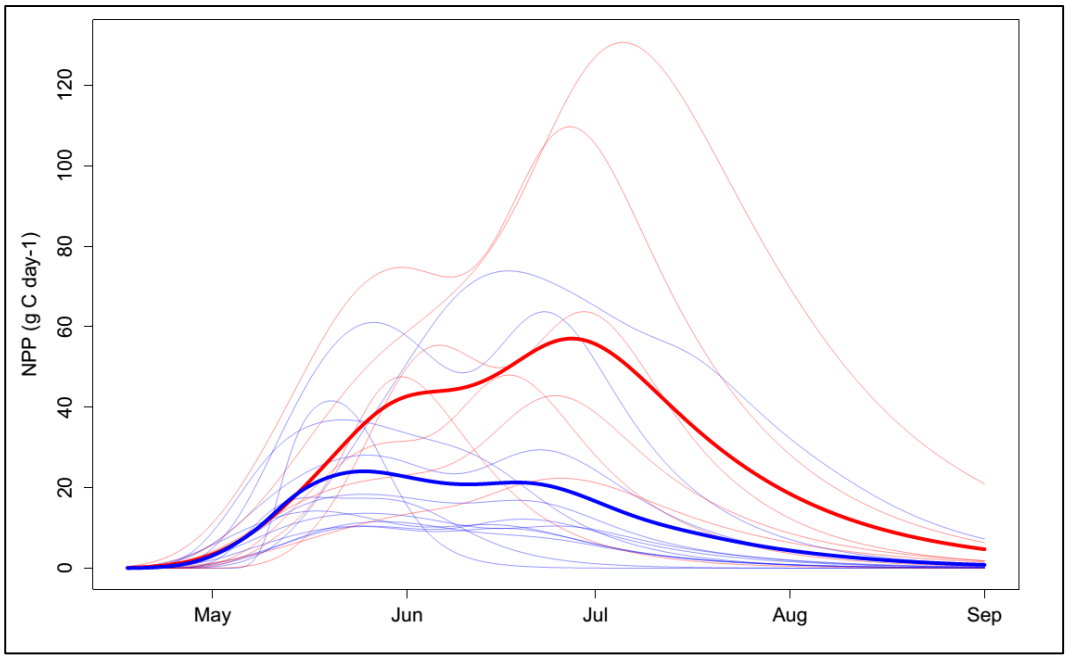

Fig 3.5. 2015 NPP by species and individual (absolute). Red lines= Douglas fir; Blue lines= Western redcedar; Thick lines=Species averages.

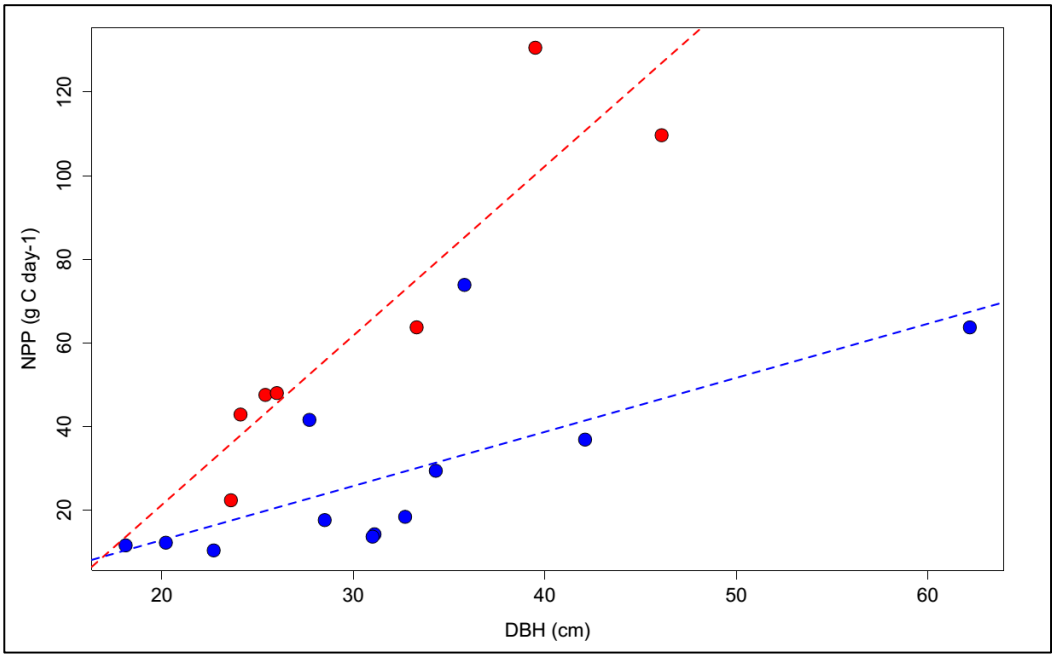

Fig 3.6. Tree NPP ~ Size relationship. Blue points=Western redcedar; Red points=Douglas fir; Blue dotted line= Western redcedar-only fitted linear model (R-squared = 0.49). Red dotted line= Douglas fir-only fitted linear model (R-squared =0.83). Note: R-squared value for the linear model including both species and DBH as predictors was 0.80, with significant relationships to NPP ($p<.05$) for DBH and DBH*Species).

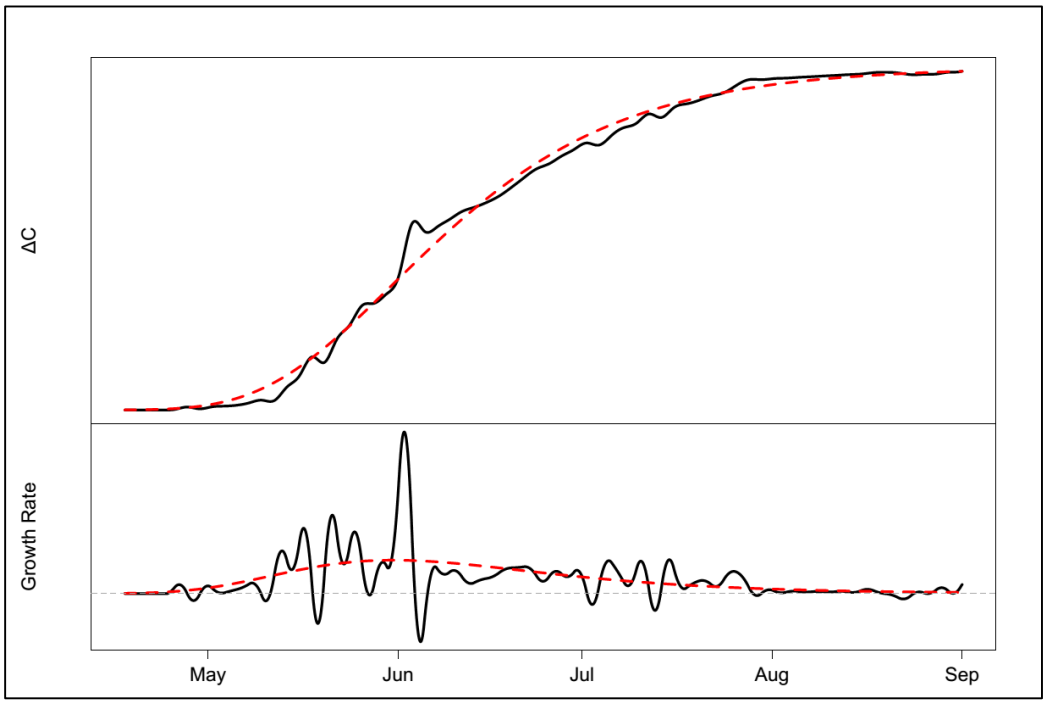

Fig 3.7. Top: Conceptual illustration of Gompertz model fit (dashed red line) to a dendrometer ΔC series (black line). Bottom: Growth rates calculated from the top panel (legend as in top panel).

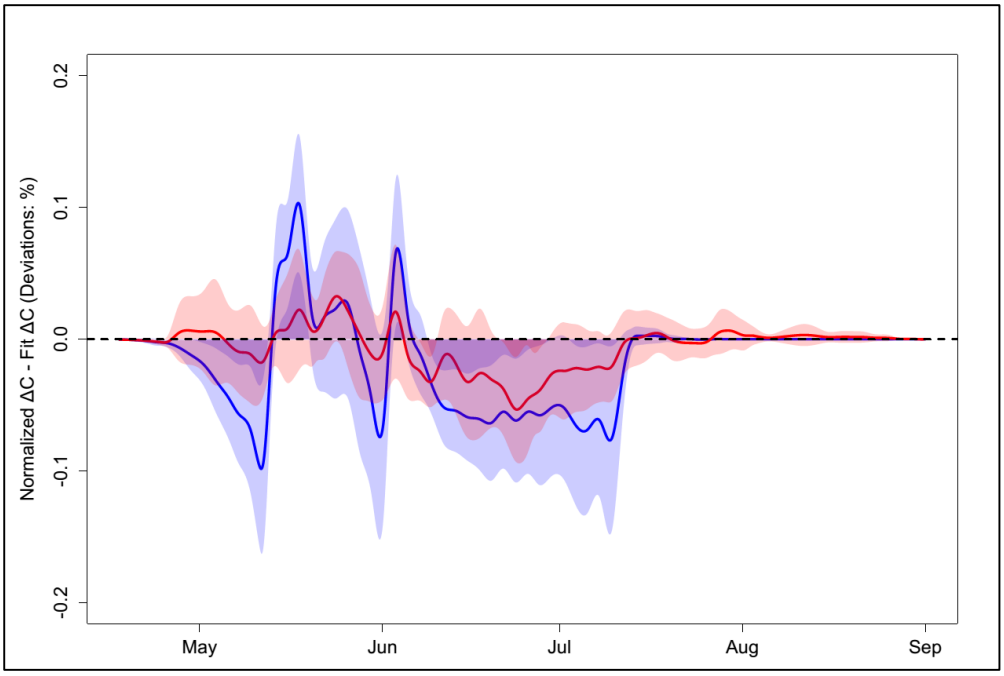

Fig 3.8. Deviations between modeled growth and normalized ΔC (ΔC – modeled). Positive values indicate measurement underperformance in comparison to modeled values. Red line=Douglas fir average deviations; red shading=Douglas fir deviation sd; blue line= Western redcedar average deviations; red shading= Western redcedar deviation sd.

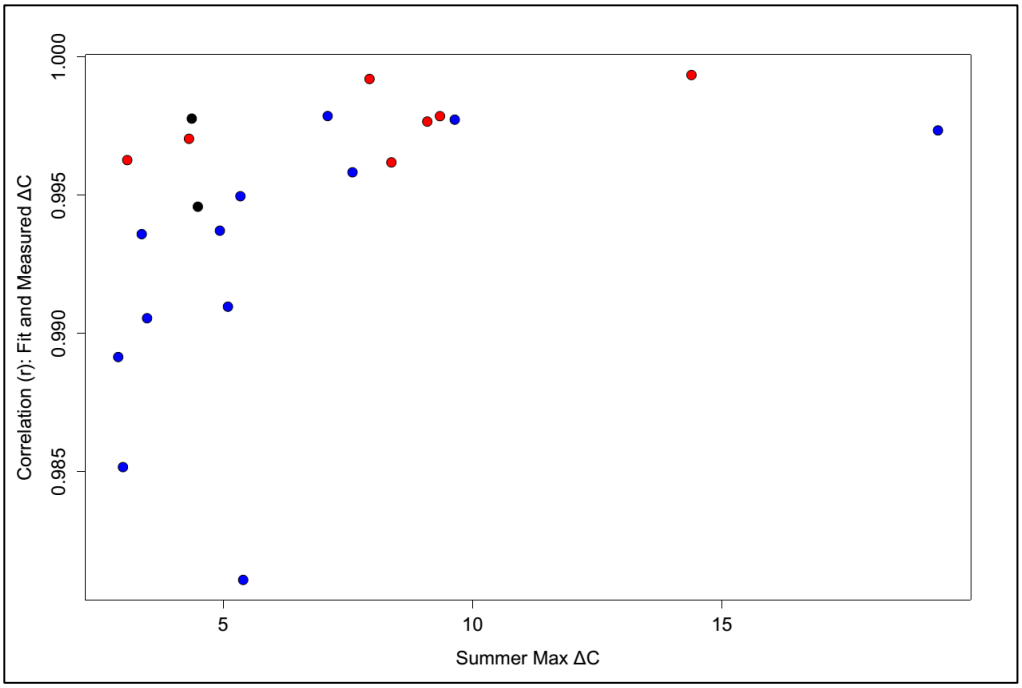

Fig 3.9. Curve fit Correlation coefficients (r) (between Gompertz fit curves and dendrometer growing season ΔC series) by dendrometer summer max ΔC. Blue points=Western redcedar; Red points=Douglas fir; Black points=Grand fir.

References

1. G. B. Bonan, Forests and climate change: forcings, feedbacks, and the climate benefits of forests. *Science (80-.).* **320**, 1444–1449 (2008).
2. M. K. Van der Molen *et al.*, Drought and ecosystem carbon cycling. *Agric. For. Meteorol.* **151**, 765–773 (2011).
3. C. D. Allen *et al.*, A global overview of drought and heat-induced tree mortality reveals emerging climate change risks for forests. *For. Ecol. Manage.* **259**, 660–684 (2010).
4. C. D. Allen, D. D. Breshears, N. G. McDowell, On underestimation of global vulnerability to tree mortality and forest die-off from hotter drought in the Anthropocene. *Ecosphere*. **6**, 1–55 (2015).
5. P. Ciais *et al.*, Europe-wide reduction in primary productivity caused by the heat and drought in 2003. *Nature*. **437**, 529–533 (2005).
6. C. R. Schwalm *et al.*, Reduction in carbon uptake during turn of the century drought in western North America. *Nat. Geosci.* **5**, 551–556 (2012).
7. B. E. Law, Regional analysis of drought and heat impacts on forests: Current and future science directions. *Glob. Chang. Biol.*, 3595–3599 (2014).
8. F. S. Chapin *et al.*, Reconciling Carbon-cycle Concepts, Terminology, and Methods. *Ecosystems*. **9**, 1041–1050 (2006).
9. M. L. Goulden, J. W. Munger, S.-M. Fan, B. C. Daube, S. C. Wofsy, Measurements of carbon sequestration by long-term eddy covariance: Methods and a critical evaluation of accuracy. *Glob. Chang. Biol.* **2**, 169–182 (1996).
10. D. D. Baldocchi, Assessing the eddy covariance technique for evaluating carbon dioxide exchange rates of ecosystems: past, present and future. *Glob. Chang. Biol.* **9**, 479–492 (2003).
11. F. Babst *et al.*, Above-ground woody carbon sequestration measured from tree rings is coherent with net ecosystem productivity at five eddy-covariance sites. *New Phytol.* **201**, 1289–1303 (2014).
12. T. Hudiburg *et al.*, Carbon Dynamics of Oregon and Northern California Forests and Potential Land-Based Carbon Storage. *Ecol. Appl.* **19**, 163–180 (2009).
13. S. M. McMahon, G. G. Parker, A general model of intra-annual tree growth using dendrometer bands. *Ecol. Evol.* **5**, 243–54 (2015).
14. S. W. Running, M. Zhao, *User's Guide: Daily GPP and Annual NPP (MOD17A2/A3) Products, NASA Earth Observing System MODIS Land Algorithm* (ed. 3.0, 2015).
15. M. Zhao, S. W. Running, Drought-Induced Reduction in Global. *Science (80-.).* **329**, 940–943 (2010).

16. C. M. Litton, J. W. Raich, M. G. Ryan, Carbon allocation in forest ecosystems. *Glob. Chang. Biol.* **13**, 2089–2109 (2007).

17. T. W. Hudiburg, B. E. Law, C. Wirth, S. Luyssaert, Regional carbon dioxide implications of forest bioenergy production. *Nat. Clim. Chang.* **1**, 419–423 (2011).

18. D. M. Drew, G. M. Downes, The use of precision dendrometers in research on daily stem size and wood property variation: A review. *Dendrochronologia*. **27**, 159–172 (2009).

19. A. Deslauriers, S. Rossi, T. Anfodillo, Dendrometer and intra-annual tree growth: What kind of information can be inferred? *Dendrochronologia*. **25**, 113–124 (2007).

20. K. Steppe, F. Sterck, A. Deslauriers, Diel growth dynamics in tree stems : linking anatomy and ecophysiology. *Trends Plant Sci.*, 1–9 (2015).

21. R. Zweifel, H. Item, R. Häsler, Stem radius changes and their relation to stored water in stems of young Norway spruce trees. *Trees*. **15**, 50–57 (2000).

22. K. Steppe, H. Cochard, A. Lacointe, T. Améglio, Could rapid diameter changes be facilitated by a variable hydraulic conductance? *Plant, Cell Environ.* **35**, 150–157 (2012).

23. R. Zweifel, H. Item, R. Häsler, Link between diurnal stem radius changes and tree water relations. *Tree Physiol.* **21**, 869–877 (2001).

24. F. Biondi, S. Rossi, Plant-water relationships in the Great Basin Desert of North America derived from Pinus monophylla hourly dendrometer records. *Int. J. Biometeorol.* **59**, 939–953 (2015).

25. J. Vieira, S. Rossi, F. Campelo, H. Freitas, C. Nabais, Seasonal and daily cycles of stem radial variation of Pinus pinaster in a drought-prone environment. *Agric. For. Meteorol.* **180**, 173–181 (2013).

26. R. Zweifel, R. Häsler, Dynamics of water storage in mature subalpine Picea abies: temporal and spatial patterns of change in stem radius. *Tree Physiol.* **21**, 561–569 (2001).

27. R. Zweifel *et al.*, Link between continuous stem radius changes and net ecosystem productivity of a subalpine Norway spruce forest in the Swiss Alps. *New Phytol.* **187**, 819–830 (2010).

28. M. Lempereur *et al.*, Growth duration is a better predictor of stem increment than carbon supply in a Mediterranean oak forest: Implications for assessing forest productivity under climate change. *New Phytol.* **207**, 579–590 (2015).

29. A. Granier, N. Bréda, B. Longdoz, P. Gross, J. Ngao, Ten years of fluxes and stand growth in a young beech forest at Hesse, North-eastern France. *Ann. For. Sci.* **65**, 704 (2008).

30. O. Bouriaud, J.-M. Leban, D. Bert, C. Deleuze, Intra-annual variations in climate influence growth and wood density of Norway spruce. *Tree Physiol.* **25**, 651–60 (2005).

31. H. E. Cuny *et al.*, Woody biomass production lags stem-girth increase by over one month in coniferous forests. *Nat. Plants*. **1**, 15160 (2015).

32. O. S. University, PRISM Climate Group, (available at http://prism.oregonstate.edu).

33. R. S. Dodd, Kinetic of Tracheid Differentiation in Douglas-fir. *Ann. Bot.* **65**, 649–657 (1990).

34. W. H. Emmingham, Comparison of selected Douglas-fir seed sources for cambial and leader growth patterns in four western Oregon environments. *Can. J. For. Res.* **7**, 154–164 (1977).

35. R. Team, R: A language and environment for statistical computing (2013) (available at http://cran.fiocruz.br/web/packages/dplR/vignettes/timeseries-dplR.pdf).

36. A. Deslauriers, H. Morin, C. Urbinati, M. Carrer, Daily weather response of balsam fir (Abies balsamea (L.) Mill.) stem radius increment from dendrometer analysis in the boreal forests of Québec (Canada). *Trees - Struct. Funct.* **17**, 477–484 (2003).

37. A. Turcotte, H. Morin, C. Krause, A. Deslauriers, M. Thibeault-Martel, The timing of spring rehydration and its relation with the onset of wood formation in black spruce. *Agric. For. Meteorol.* **149**, 1403–1409 (2009).

38. F. Tardieu, B. Parent, C. F. Caldeira, C. Welcker, Genetic and physiological controls of growth under water deficit. *Plant Physiol.* **164**, 1628–35 (2014).

39. J. Tardif, M. Flannigan, Y. Bergeron, An analysis of the daily radial activity of 7 boreal tree species, northwestern Quebec. *Environ. Monit. Assess.* **67**, 141–160 (2001).

40. H. Abe, T. Nakai, Y. Utsumi, A. Kagawa, Temporal water deficit and wood formation in Cryptomeria japonica. *Tree Physiol.* **23**, 859–863 (2003).

41. T. C. Hsiao, Plant Responses To Water Stress. *Annu. Rev. Plant Physiol.* **24**, 519–570 (1973).

42. J. J. Camarero, J. M. Olano, A. Parras, Plastic bimodal xylogenesis in conifers from continental Mediterranean climates. *New Phytol.* **185**, 471–480 (2010).

43. H. E. Cuny, C. B. K. Rathgeber, D. Frank, P. Fonti, M. Fournier, Kinetics of tracheid development explain conifer tree-ring structure. *New Phytol.* **203**, 1231–1241 (2014).

44. J. P. Lassoie, Stem Dimensional Fluctuations in Douglas-fir of Different Crow Classes. *For. Sci.* **25**, 132–144 (1979).

45. R. H. Waring, S. W. Running, Sapwood water storage:its contribution to transpiration and effect upon water conductance through te stems of old growth Douglas fir. *Plant, Cell Environ.* **1**, 131–140 (1978).

46. J. Cermak, J. Kucera, W. L. Bauerle, N. Phillips, T. M. Hinckley, Tree water storage and its diurnal dynamics related to sap flow and changes in stem volume in old-growth Douglas-fir trees. *Tree Physiol.* **27**, 181–198 (2007).

47. N. G. Phillips *et al.*, Reliance on stored water increases with tree size in three species in the Pacific Northwest. *Tree Physiol.* **23**, 237–245 (2003).

48. S. Rossi *et al.*, Conifers in cold environments synchronize maximum growth rate of tree-ring formation with day length. *New Phytol.* **170**, 301–310 (2006).

49. F. Campelo, C. Nabais, H. Freitas, E. Gutierrez, Climatic significance of tree-ring width and intra-annual density fluctuations in Pinus pinea from a dry Mediterranean area in Portugal. *Ann. For. Sci.* **64**, 229–238 (2007).

50. N. Delpierre, D. Berveiller, E. Granda, E. Dufrêne, Wood phenology, not carbon input, controls the interannual variability of wood growth in a temperate oak forest. *New Phytol.*, 459–470 (2015).

51. R. Zweifel, L. Zimmermann, F. Zeugin, D. M. Newbery, Intra-annual radial growth and water relations of trees: implications towards a growth mechanism. *J. Exp. Bot.* **57**, 1445–59 (2006).

52. P. A. Beedlow, E. H. Lee, D. T. Tingey, R. S. Waschmann, C. A. Burdick, The importance of seasonal temperature and moisture patterns on growth of Douglas-fir in western Oregon, USA. *Agric. For. Meteorol.* **169**, 174–185 (2013).

53. F. Babst *et al.*, Site- and species-specific responses of forest growth to climate across the European continent. *Glob. Ecol. Biogeogr.* **22**, 706–717 (2013).

54. R. Savidge, Xylogenesis, genetic and environmental regulation-a review. *Iawa J.* (1996) (available at http://booksandjournals.brillonline.com/content/journals/10.1163/22941932-90001580).

55. P. Ren, S. Rossi, J. Gricar, E. Liang, K. Cufar, Is precipitation a trigger for the onset of xylogenesis in Juniperus przewalskii on the north-eastern Tibetan Plateau? *Ann. Bot.* **115**, 629–639 (2015).

56. S. Rossi *et al.*, Critical temperatures for xylogenesis in conifers of cold climates. *Glob. Ecol. Biogeogr.* **17**, 696–707 (2008).

57. F. Babst *et al.*, Blue intensity parameters derived from Ponderosa pine tree rings characterize intra-annual density fluctuations and reveal seasonally divergent water limitations. *Trees - Struct. Funct.*, 1–13 (2016).

58. F. Babst, D. C. Frank, U. Büntgen, D. Nievergelt, J. Esper, Effect of sample preparation and scanning resolution on the Blue Reflectance of Picea abies. *TRACE–Tree Rings Archaeol. Climatol. Ecol.* **7**, 188–195 (2009).

59. R. Campbell *et al.*, Blue Intensity In Pinus sylvestris Tree Rings: A Manual for A New Palaeoclimate Proxy. *Tree-Ring Res.* **67**, 127–134 (2011).

60. W. S. Rasband, ImageJ (1997).

61. Z. Pödör, M. Manninger, L. Jereb, in *Advanced Computational Methods for* (2014; http://link.springer.com/chapter/10.1007/978-3-319-06569-4_26), pp. 353–364.

62. S. Rossi, T. Anfodillo, R. Menardi, Trephor: A new tool for sampling microcores from tree stems. *IAWA J.* **27**, 89–97 (2006).

Appendix A

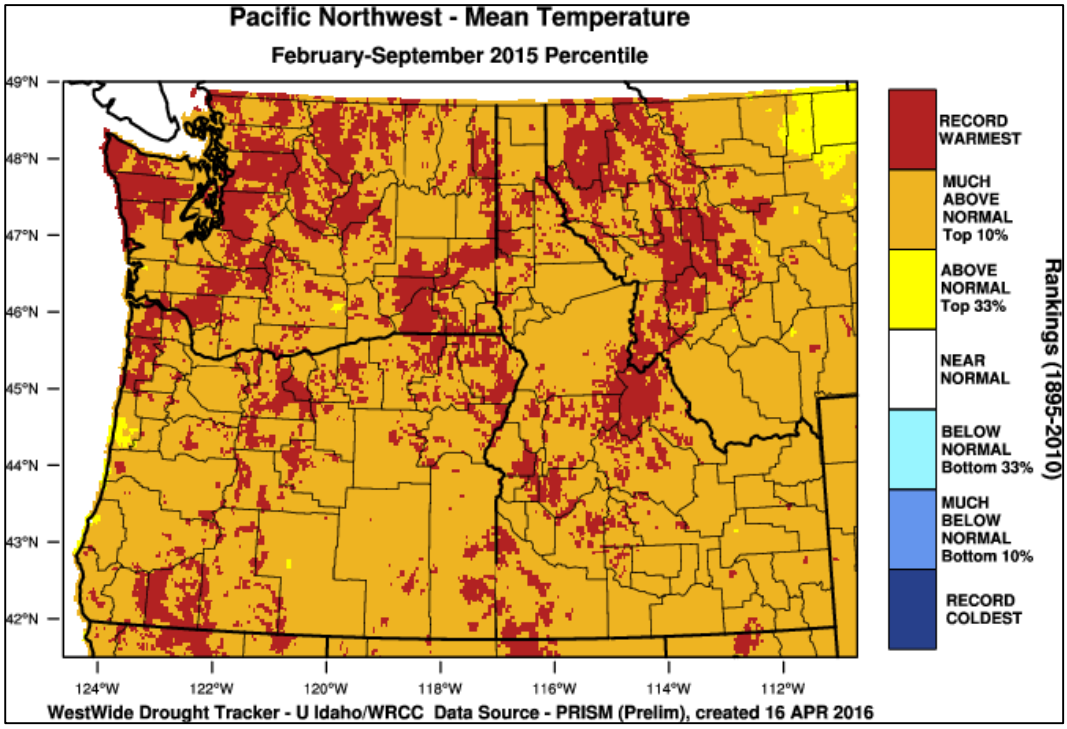

Figure A.1. February-September 2015 NW U.S. temperature comparison to historical period. Created with WestWide Drought Tracker web tool (WWDT; http://www.wrcc.dri.edu/wwdt/index.php); interpolated data from PRISM Climate Mapping Program.

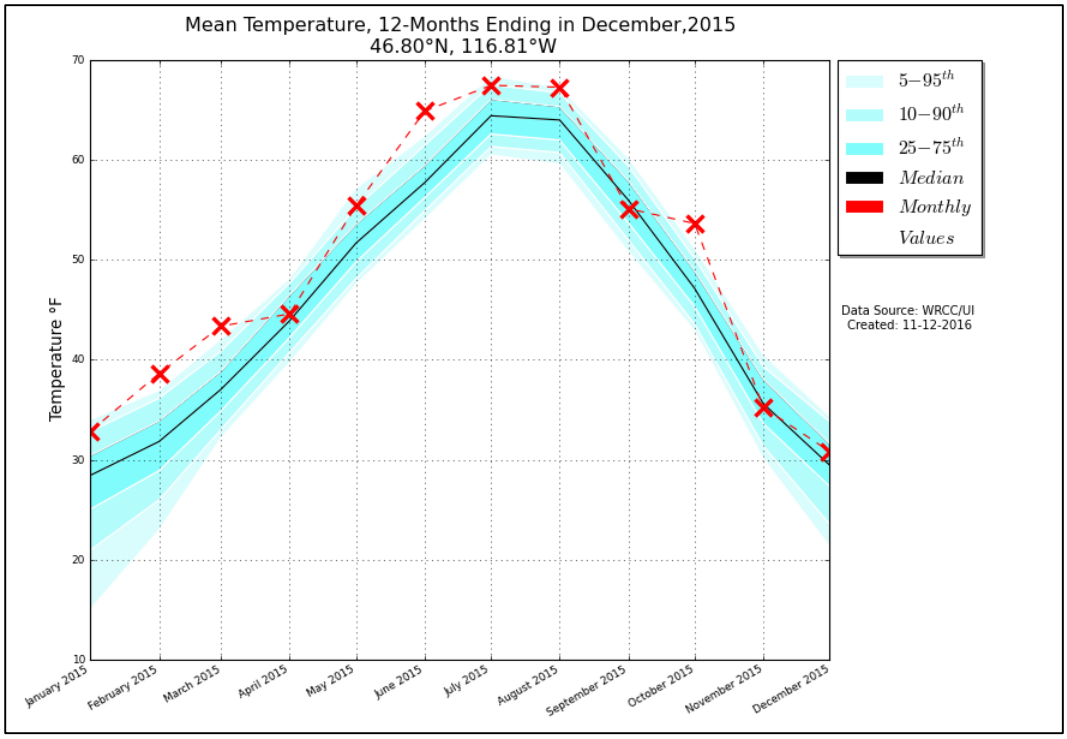

Figure A.2. 2015 Monthy site temperatures commpared to 1981-2010 values. (Created with WWDT)

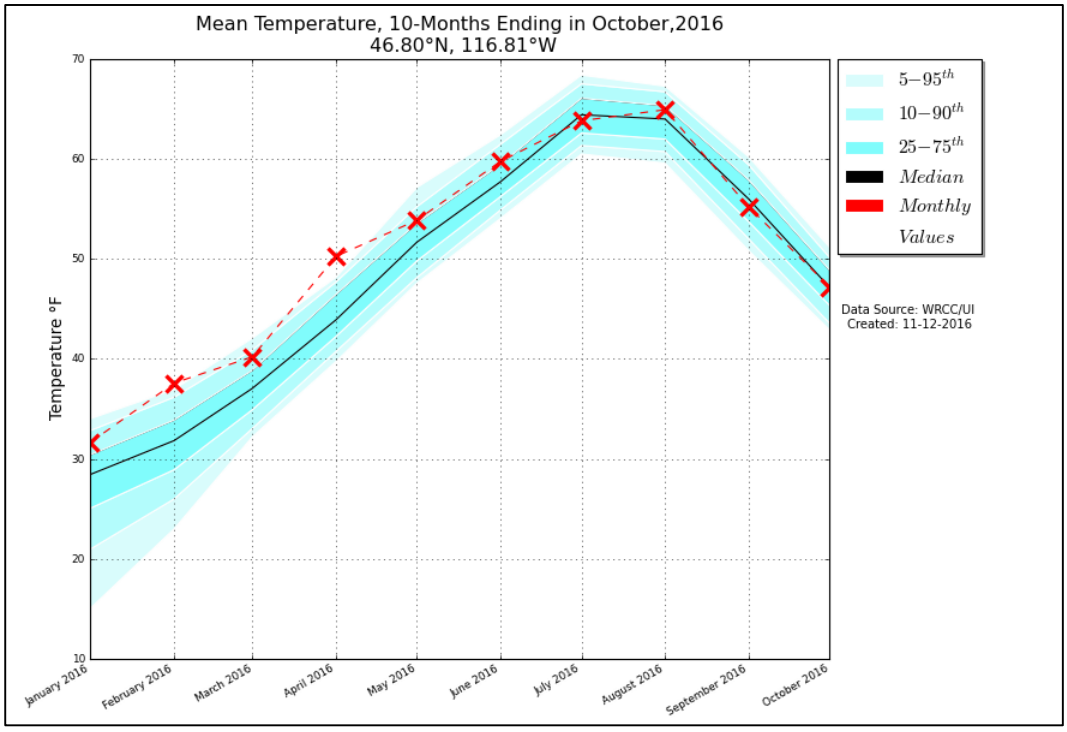

Figure A.3. 2016 Monthy site temperatures commpared to 1981-2010 values (Created with WWDT).

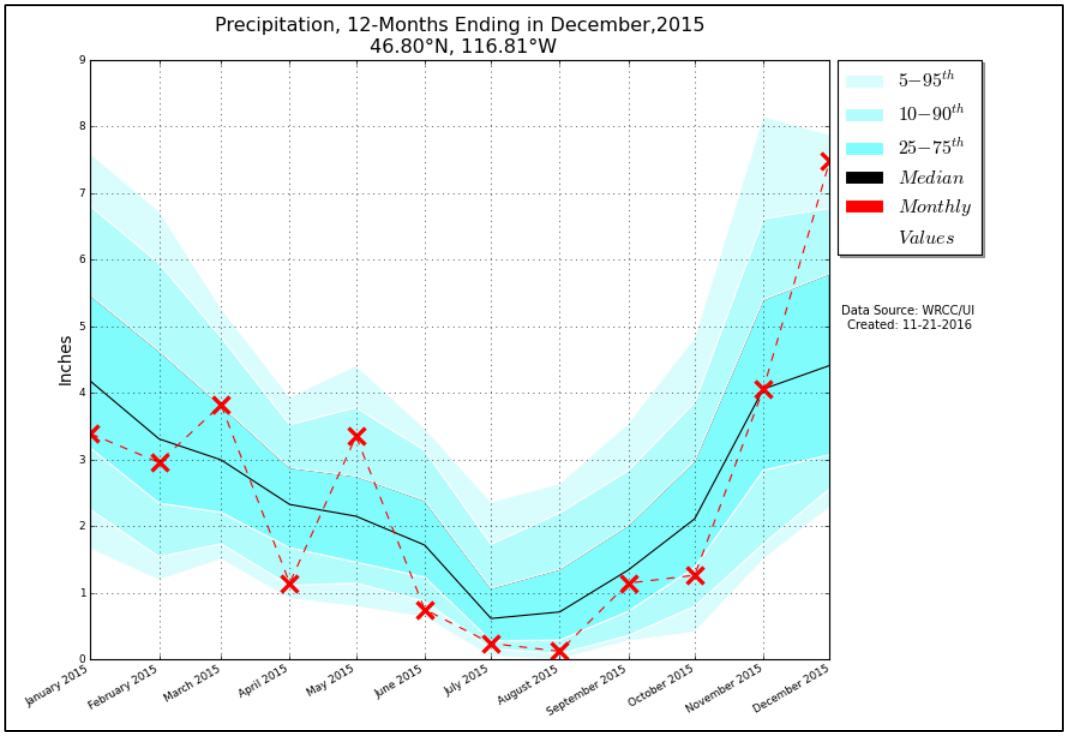

Figure A.4. 2015 Monthy site precipitation commpared to 1981-2010 values (Created with WWDT).

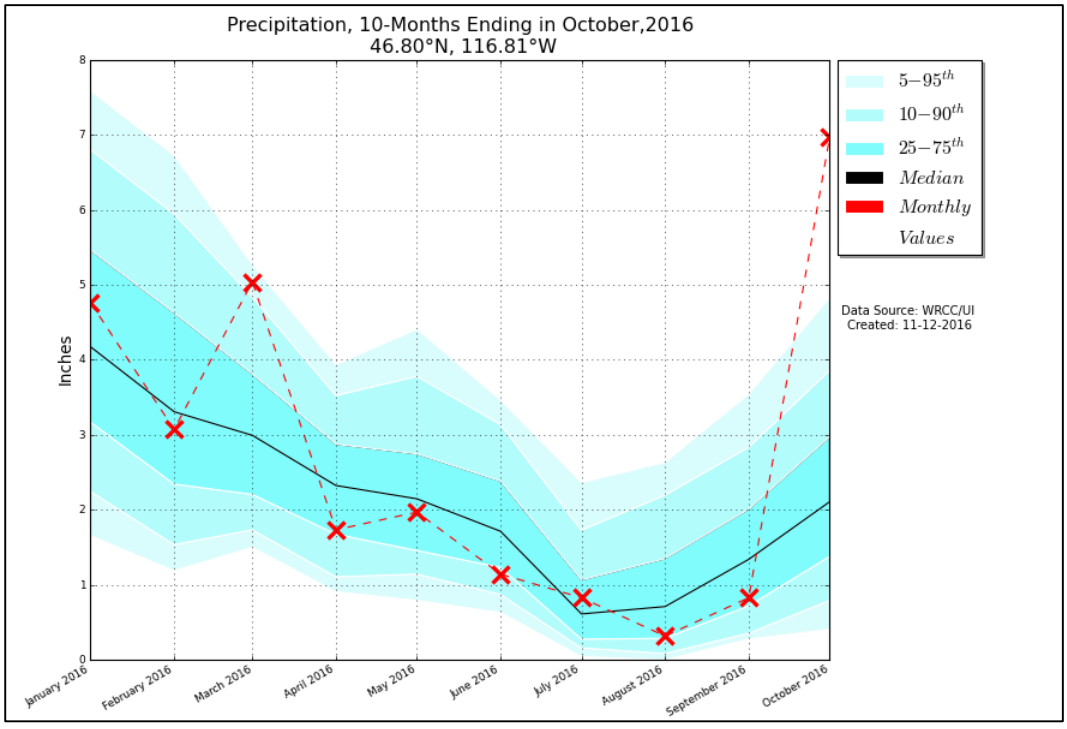

Figure A.5. 2015 Monthy site precipitation commpared to 1981-2010 values (Created with WWDT).

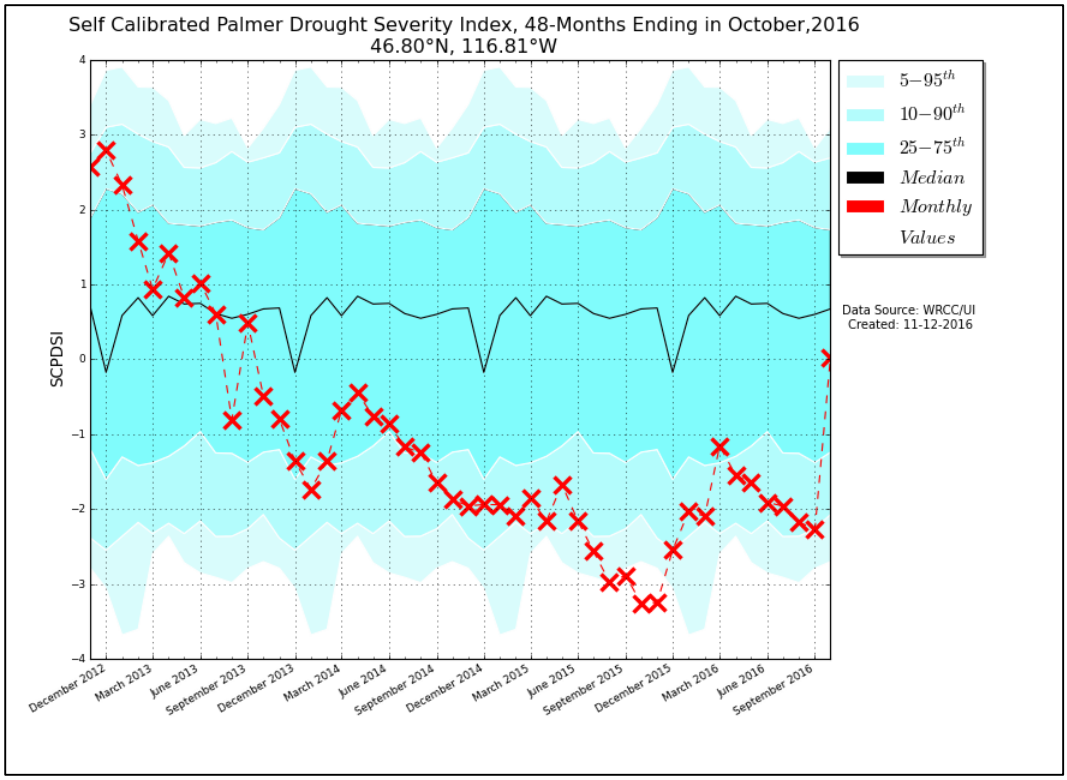

Figure A.6. 48 month sc-PSCI Ending in October 2016 compared to 1981-2010 values.